Vehicle Energy Consumption

A contribution to the Coherent Energy and Environmental System Analysis (CEESA) project

Schaltz, Erik

Publication date:
2011

Document Version
Publisher's PDF, also known as Version of record

Department of
ENERGY TECHNOLOGY
E.T.

Vehicle Energy Consumption

- A contribution to the Coherent Energy and Environmental System Analysis (CEESA) project

by

Erik Schaltz

Department of Energy Technology, Aalborg University
Aalborg, Denmark, January 18, 2011

Abstract

In this report simulation models of a Battery Electric Vehicle (BEV) and a Fuel Cell Hybrid Electric Vehicle (FCHEV) have been developed. The models have two features: they both design the vehicles and calculates the energy consumption, efficiency, mass, volume, and cost due to a given drive cycle. The vehicles are designed to fulfill a drive cycle which consist of city, road, and motorway driving, as it is desired that the vehicles should have the same performance as traditional internal combustion engine (ICE) vehicles. For this reason its also chosen to use a midsize car, i.e. a Toyota Avensis, as reference vehicle. The simulation models consist of several sub-models, which have been modeled by use of data sheets. The models have therefore not been verified be experimental results, which is strongly recommenced for future work.

The energy consumption per km and efficiency are significant better for the BEV than for the FCHEV. The average energy consumption per km is $304.1\,\mathrm{Wh/km}$ and $635.7\,\mathrm{Wh/km}$ for the BEV and FCHEV, respectively. The average tank-to-wheel efficiency of the BEV and FCHEV are $54.0\,\%$ and $23.4\,\%$, respectively. For the total car mass and cost and volume of the power system, the results are two-sided. For short distance the BEV is lighter, has smaller volume of the power system, and are cheaper than the FCHEV. However, when the traveling distance increases the difference becomes smaller, and at long distances the FCHEV are the lightest, smallest, and cheapest.

Nomenclature

BEV Battery Electric Vehicle
CEESA Coherent Energy and Environmental System Analysis
FCHEV Fuel cell Hybrid Electric Vehicle
HVAC Heating Ventilation Air Condition
ICE Internal Combustion Engine
IM Induction Machine
LiIon Lithium Ion
LTPEMFC Low Temperature Proton Exchange Membrane Fuel Cell
PMSM Permanent Magnet Synchronous Machine
PWM Pulse Width Modulation
SRM Switched Reluctance Machine

Contents

Abstract **iii**

Contents **vi**

1 Introduction **1**
1.1 Purpose 1
1.2 Driving Cycle 1
1.3 Reference Vehicle 1

2 Vehicle Modeling **5**
2.1 Vehicle Force Model 5
2.2 Electric Loads 6
2.3 Battery Electric Vehicle 6
2.4 Fuel Cell Hybrid Electric Vehicle 14
2.5 Key Figures 16
2.6 Simulation Results 19

3 Conclusion **25**

Bibliography **27**

A Battery **29**
A.1 Specifications and Characteristics 29
A.2 Modeling 29
A.3 Cycle efficiency 40

B Electric Machine **43**
B.1 Modeling 43
B.2 Design 45

C Transmission **51**

D Inverter **53**

E Rectifier **57**
E.1 Design 60

F Boost Converter **61**
F.1 Design 61

G Braking Resistor **63**

H Fuel Cell Modeling **65**
H.1 Specifications and Characteristics 65
H.2 Polarization Curve Modeling 65
H.3 Efficiency Modeling 66

1 Introduction

In this chapter the purpose, driving cycle, and reference vehicle are given.

1.1 Purpose

The CEESA project investigates the challenges of the future sustainable energy system. A significant challenge is to integrate the transportation sector in the energy system.

In this report different types of vehicles are analyzed in order to be able to calculate their energy consumption.

1.2 Driving Cycle

A very important issue is the selection of driving cycle as it determines the energy and power requirement. Several different kind of vehicles will be investigated, and it is therefore important that the driving cycle is realistic so it does not favor one specific kind of vehicle, e.g. it is expected that a hybrid vehicle will perform well in a city environment with low speed and many stop-and-goes, due to the regenerative braking. A traditional vehicle with internal combustion engine (ICE) cannot utilize the kinetic energy when braking, and it is therefore expected that a vehicle with an ICE will have a higher energy consumption in city driving. However, at motorway speed there is very limited regenerative braking and the difference in fuel consumption is therefore expected to be smaller.

In order to have a realistic driving cycle it is chosen to create a driving cycle with three different environments, i.e. urban driving, road driving, and motorway driving. In Figure 1.1(a-c) an Artemis urban, road, and motorway driving cycle are shown. The three cycles are merged together in Figure 1.1(d) where they create a fourth driving cycles. The red vertical lines indicates how the three Artemis driving cycles are combined. In Table 1.1 is shown the key numbers of the four driving cycles.

1.3 Reference Vehicle

The type of car will strongly affect the energy consumption of the vehicle, i.e. the energy consumption is usually better for a small car than for a big four wheel drive truck. In 2009 Toyota Avensis was the most sold car with 3265 newly registered cars

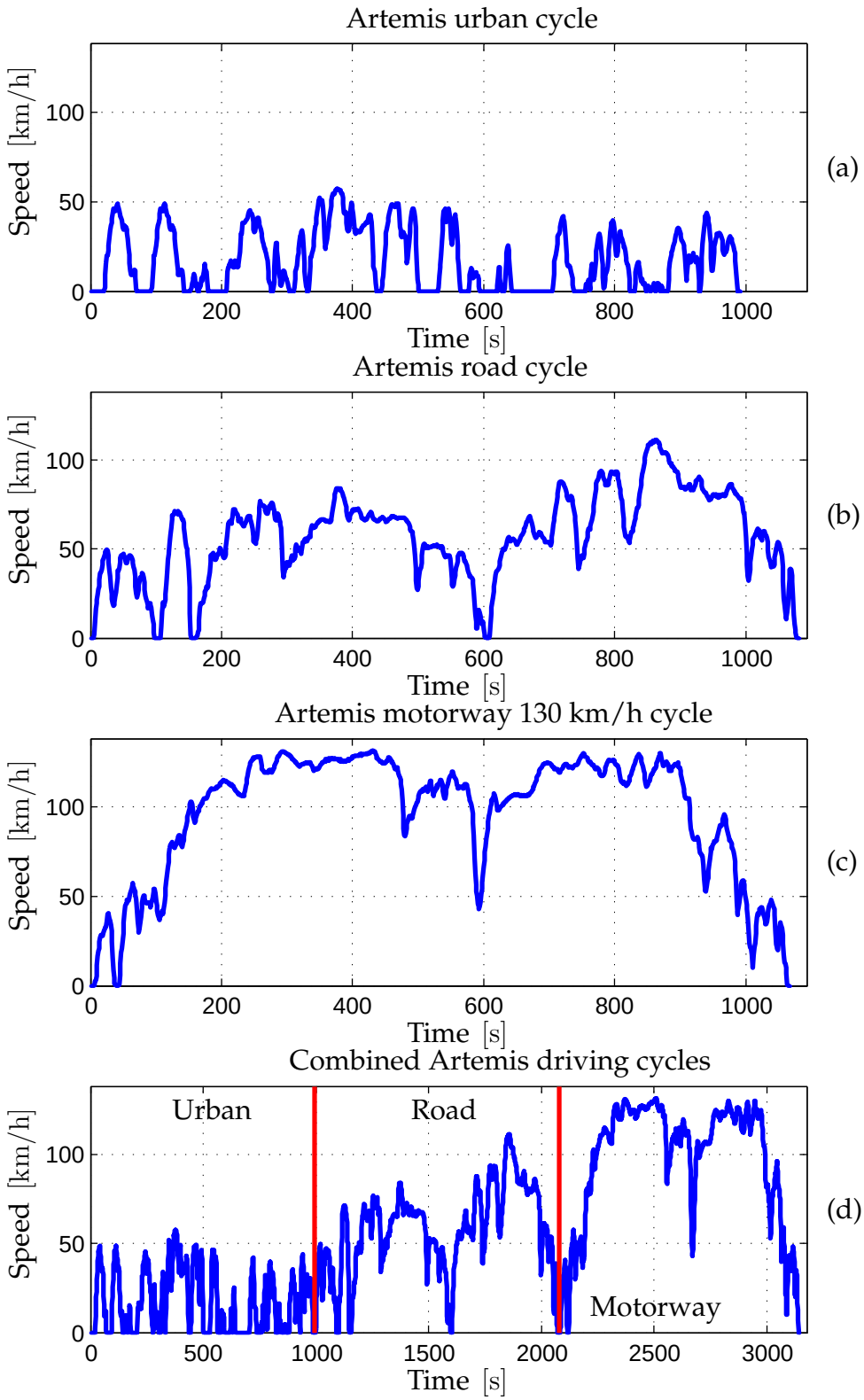

Figure 1.1: Artemis driving cycles. (a) Urban cycle. (b) Road cycle. (c) Motorway cycle. (d) Combined driving cycles.

		Urban	Road	Motorway	Combined
Duration	[s]	993	1082	1068	3145
Distance	[km]	4.87	17.27	28.74	50.88
Maximum speed	[km/h]	57.7	111.5	131.8	131.8
Average speed	[km/h]	17.65	57.47	96.86	58.24

Table 1.1: Key numbers of Artemis driving cycles.

[4] and this car is therefore selected as a reference car as it is a medium size car which full fills most purposes of a general family.

According to the home page of Toyota [17] is the sedan model "1.6 VVT-i 6 M/T" able to go from $0\,\mathrm{km/h}$ to $100\,\mathrm{km/h}$ in $10.4\,\mathrm{s}$ and it has a maximum speed of $200\,\mathrm{km/h}$.

Vehicle Parameters

The tires of the Toyota Avensis have the code "205/60R16" [17] which means that they are $l_w = 205\,\mathrm{mm}$ wide, the hight of the tires is 60% of the width, and that the diameter of the felloes is $d_f = 16\,\mathrm{in}$ [16]. The wheel radius is therefore given by

$$r_\mathrm{w} = \frac{d_f \cdot 0.0254\,\mathrm{m/in} + 2 \cdot l_w \cdot 0.60 \cdot 0.001\,\mathrm{m/mm}}{2} = 0.33\,\mathrm{m} \tag{1.1}$$

The aerodynamic drag coefficient and front area are not specified on the Toyota website. For the aerodynamic drag coefficient $C_\mathrm{drag} = 0.3$ is chosen as this is suitable for a type similar to the Avensis (Wedge-shaped) [5]. An area of $A_\mathrm{front} = 2.27\,\mathrm{m}^2$ is selected as this is a typical for a midsize sedan [14]. The curb weight of the Avensis is $1475\,\mathrm{kg}$ [17], but the glider mass is not specified. In [14] is a midsize sedan with a curb mass of $1429\,\mathrm{kg}$ specified to have a glider mass of $905\,\mathrm{kg}$. As the two curb masses are quite similar is it chosen to use a glider mass of $M_\mathrm{glider} = 905\,\mathrm{kg}$.

Toyota specifies the cost of the car to be $\mathrm{Cost}_\mathrm{Avensis,incl,TAX} = 285,953\,\mathrm{DKK}$ including VAT and registration tax. According to Skatteministeriet is the registration tax given by [15]:

- 105% tax below $79,000\,\mathrm{DKK}$
- 180% tax above $79,000\,\mathrm{DKK}$
- $1000\,\mathrm{DKK}$ tax reduction for each kilometer per liter the fuel consumption is higher than $16\,\mathrm{km/L}$
- $1000\,\mathrm{DKK}$ tax addition for each kilometer per liter the fuel consumption is lower than $16\,\mathrm{km/L}$

The Toyota Avensis has a fuel consumption of $15.4\,\mathrm{km/L}$ [17] which means that the tax due to the fuel consumption alone $\mathrm{TAX}_\mathrm{fuel}$ is

$$\mathrm{TAX}_\mathrm{fuel} = 1000\,\mathrm{DKK/(km/L)} \cdot (16\,\mathrm{km/L} - 15.4\,\mathrm{km/L}) = 600\,\mathrm{DKK} \tag{1.2}$$

The cost of the Avensis without registration tax (but with VAT) $\text{Cost}_{\text{Avensis,incl,VAT}}$ is therefore

$$\begin{aligned}\text{Cost}_{\text{Avensis,incl,TAX}} &= \text{Cost}_{\text{Avensis,incl,VAT}} + 1.05 \cdot 79,000\,\text{DKK} \\ &\quad + 1.8 \cdot (\text{Cost}_{\text{Avensis,incl,VAT}} - 79,000\,\text{DKK}) \\ &\quad + \text{TAX}_{\text{fuel}} \qquad [\text{DKK}] \end{aligned} \tag{1.3}$$

$$\Updownarrow$$

$$\begin{aligned}\text{Cost}_{\text{Avensis,incl,VAT}} &= \frac{\text{Cost}_{\text{Avensis,incl,TAX}} + 0.75 \cdot 79,000\,\text{DKK}}{2.8} \\ &\quad - \frac{\text{TAX}_{\text{fuel}}}{2.8} \\ &= 123,073\,\text{DKK} \end{aligned} \tag{1.4}$$

The cost of the Avensis without VAT (25%) is therefore

$$\text{Cost}_{\text{Avensis,excl,VAT}} = \frac{\text{Cost}_{\text{Avensis,incl,VAT}}}{1.25} = 98,458\,\text{DKK} \tag{1.5}$$

In [14] the glider cost is assumed to be $\frac{17{,}390\,\text{USD}}{23{,}392\,\text{USD}} = 0.74$ of the manufacturer's suggested retail price. With a price of $567.36\,\text{DKK}$ for $100\,\text{USD}$ (December 29, 2010) is the glider cost of the Toyota Avensis therefore calculated to

$$\text{Cost}_{\text{glider}} = 0.74 \frac{\text{Cost}_{\text{Avensis,excl,VAT}}}{5.6736\,\text{DKK/USD}} = 12,842\,\text{USD} \tag{1.6}$$

Summary

For simulation the parameters in Table 1.2 are used.

Wheel radius	r_{w}	$0.33\,\text{m}$
Aerodynamic drag coefficient	C_{drag}	0.3
Front area	A_{front}	$2.27\,\text{m}^2$
Glider mass	M_{glider}	$905\,\text{kg}$
Glider cost	$\text{Cost}_{\text{glider}}$	$12,842\,\$$

Table 1.2: Parameters of the vehicle.

2 Vehicle Modeling

In this chapter a Battery Electric Vehicle (BEV) and a Fuel cell Hybrid Electric Vehicle (FCHEV) will be modeled. The models makes it possible to simulate the consumed "fuel" of the vehicles due to the driving cycles presented in the previous chapter. The vehicle models also include mass, volume, and cost for each sub-model of the overall vehicle model.

2.1 Vehicle Force Model

An often used approached is to setup a free body diagram of the vehicle. When one knows the forces affecting the vehicle, it is thereby possible to calculate the required shaft torque and power to a specific time. In Figure 2.1, the forces acting on the vehicle can be seen. The forces which the motors of the vehicle must be overcome are the forces due to gravity, wind, rolling resistance, and inertial effect.

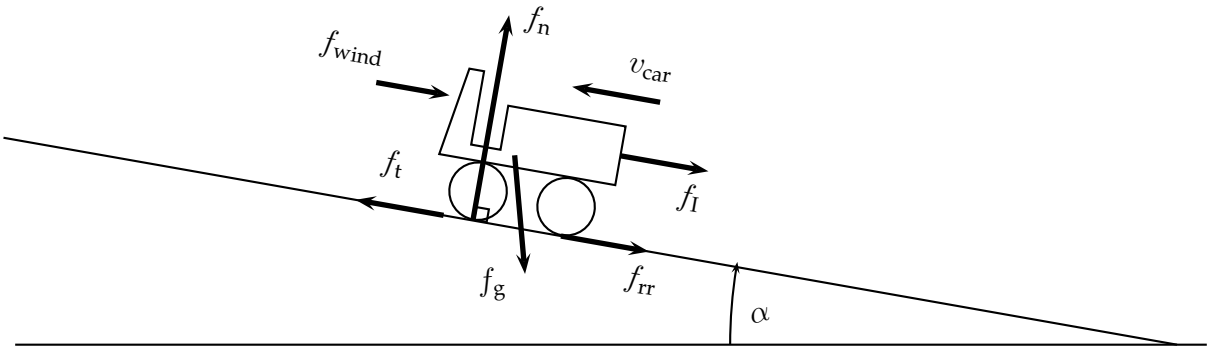

Figure 2.1: Forces acting on the car.

The traction force of a vehicle can be described by the following two equations [5]:

$$f_{\text{t}} = \underbrace{M_{\text{car}}\dot{v}_{\text{car}}}_{f_{\text{I}}} + \underbrace{M_{\text{car}} \cdot g}_{f_{\text{g}}} \cdot \sin(\alpha) + \text{sign}(v_{\text{car}}) \overbrace{\underbrace{M_{\text{car}} \cdot g \cdot \cos(\alpha)}_{f_{\text{rr}}}}^{f_{\text{n}}} \cdot c_{\text{rr}} + \text{sign}(v_{\text{car}} + v_{\text{wind}}) \underbrace{\frac{1}{2}\rho_{\text{air}} C_{\text{drag}} A_{\text{front}} \left(v_{\text{car}} + v_{\text{wind}}\right)^2}_{f_{\text{wind}}} \tag{2.1}$$

$$c_{\text{rr}} = 0.01 \left(1 + \frac{3.6}{100} v_{\text{car}}\right) \tag{2.2}$$

where	f_{t}	$[\text{N}]$	Traction force of the vehicle
	f_{I}	$[\text{N}]$	Inertial force of the vehicle
	f_{rr}	$[\text{N}]$	Rolling resistance force of the wheels
	f_{g}	$[\text{N}]$	Gravitational force of the vehicle
	f_{n}	$[\text{N}]$	Normal force of the vehicle
	f_{wind}	$[\text{N}]$	Force due to wind resistance
	α	$[\text{rad}]$	Angle of the driving surface
	M_{car}	$[\text{kg}]$	Mass of the vehicle
	v_{car}	$[\text{m/s}]$	Velocity of the vehicle
	$\dot{v}_{\text{car}}$	$[\text{m/s}^2]$	Acceleration of the vehicle
	$g = 9.81$	$[\text{m/s}^2]$	Free fall acceleration
	$\rho_{\text{air}} = 1.2041$	$[\text{kg/m}^3]$	Air density of dry air at $20\,^{\circ}\text{C}$
	c_{rr}	$[-]$	Tire rolling resistance coefficient
	C_{drag}	$[-]$	Aerodynamic drag coefficient
	A_{front}	$[\text{m}^2]$	Front area
	v_{wind}	$[\text{m/s}]$	Headwind speed

2.2 ELECTRIC LOADS

The main purpose of the motor is to provide power for the wheels. However, a modern car have also other loads which the motor should supply. These loads are either due to safety, e.g. light, wipers, horn, etc. and/or comfort, e.g. radio, heating, air conditioning, etc. These loads are not constant, e.g. the power consumption of the air conditioning system strongly depend on the surrounding temperature. Even though some average values are suggested. These can be seen in Table 2.1. From the table it may be understood that the total average power consumption is $p_{\text{Aux}} = 957\,\text{W}$.

2.3 BATTERY ELECTRIC VEHICLE

The components of the BEV can be seen in Figure 2.2. The main components are the transmission, electric machine, inverter, battery, boost converter, active rectifier, and the grid.

Description	Average power [W]
Radio	52
Heating Ventilation Air Condition (HVAC)	489
Lights	316
Electric power steering	100
Total p_{Aux}	957

Table 2.1: The electric loads with the highest average consumption. The values are inspired from [5, 6, 9].

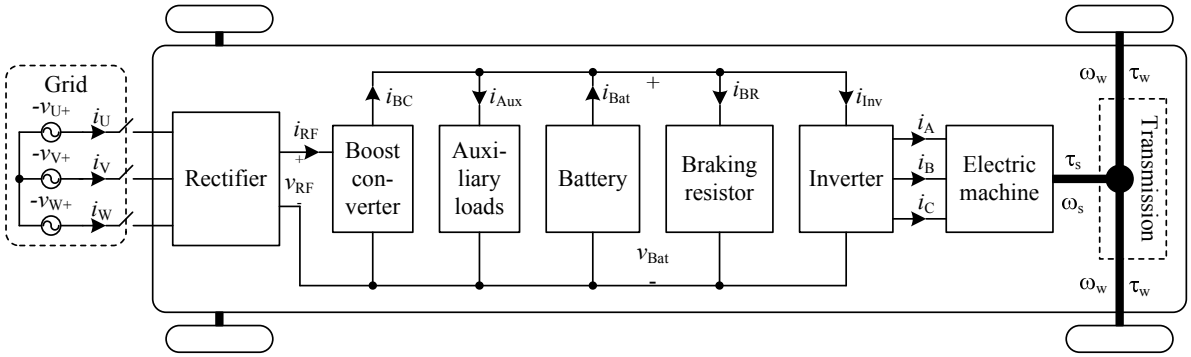

Figure 2.2: Main components of the BEV.

Main Vehicle Components

For propulsion usually the induction machine (IM), permanent magnet synchronous machine (PMSM), and switched reluctance machines (SRM) are considered. The "best" choice is like many other components a trade of between, cost, mass, volume, efficiency, reliability, maintenance, etc. However, due its high power density and high efficiency the PMSM is selected. The modeling and design of the electric machine can be seen in Appendix B.

A traditional ICE has only a high torque in a very small range of the speed. Therefore it is necessary to use a gear-box, to insure that a sufficient torque is present at the driving wheels. An electric machine provides a high torque in a wide speed range, and it is for this reason not necessary with a gear-box. However, in order to be able to operate the electric motor at a point where it has a high efficiency it might be appropriate to include a gear-box. For the same power rating an electric motor is smaller in size and weight than an ICE, and an electric motor could therefore be connected directly to all or some of the wheels of the car, which will eliminate the need for a transmission system. For simplicity it is chosen to use the conventional way, i.e. the power of the motor is fed to the two driving wheels through a differential. The modeling of the transmission system can be seen in Appendix C.

The inverter performs the conversion of the DC voltages and currents of the bus and the AC voltages and currents of the electric machine. The inverter modeling can be seen in Appendix D.

The rectifier rectifies the AC grid voltage and current to DC levels. The description of the rectifier can be seen in Appendix E.

The boost converter converts the "low" voltage of the rectifier or fuel cell to the higher bus-level. The modeling of the boost converter can be seen in Appendix F.

According to the data sheet of the battery is the maximum allowed cell voltage $V_{\text{Bat,max,cell}} = 4.2\,\text{V}$ [13]. During the regenerative braking is it therefore important that this maximum cell voltage not is exceeded. For this reason a braking resistor is introduced as it also can be seen in Figure 2.2. The modeling of the braking resistor can be seen in Appendix G.

Simulation Model

The overall vehicle model includes the model of the forces acting on the vehicle (wind, gravity, rolling resistance, etc.), and the individual components of the power train, i.e. transmission, electric machine, inverter, battery, boost converter, rectifier. The block diagram of the overall vehicle model can be seen in Figure 2.3. The wind speed v_{wind} and road angle α have been put to zero for simplicity. The simulation model has been implemented in Matlab/Simulink.

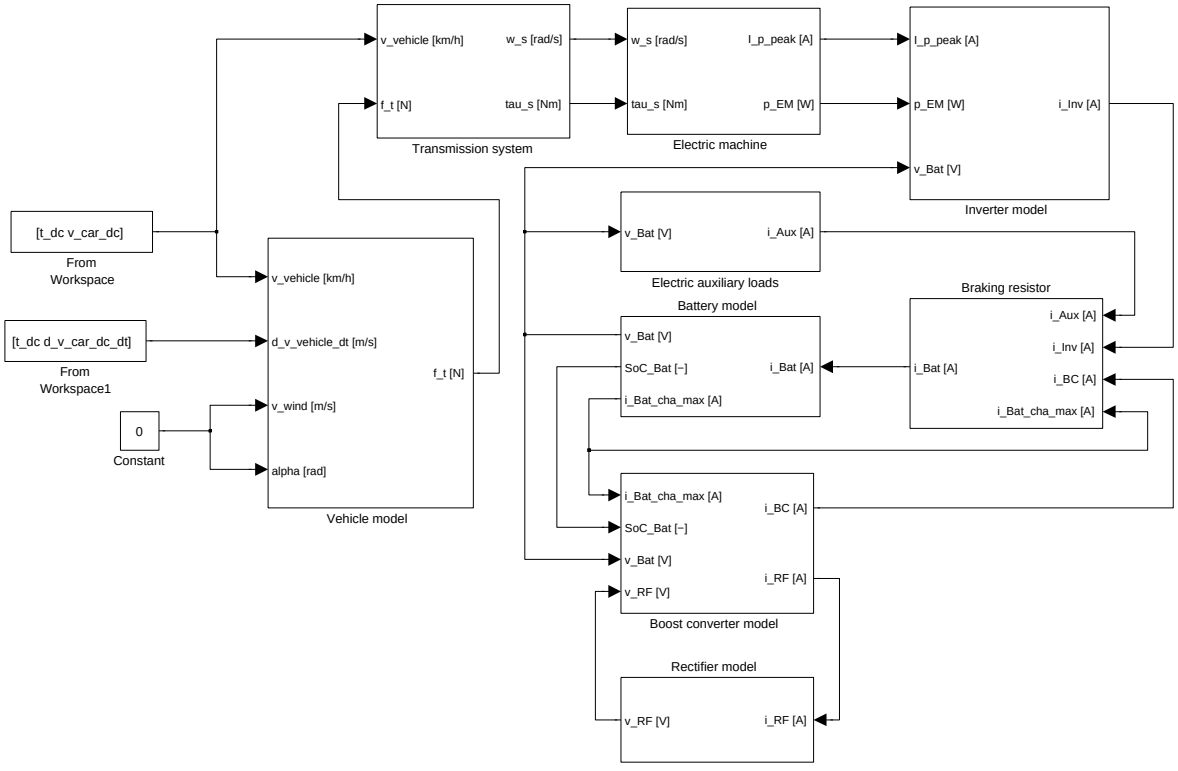

Figure 2.3: Simulink model of the BEV.

Battery Charging Control

During the charging of the battery the battery terminal voltage v_{Bat} should not exceed $V_{\text{Bat,max,cell}} = 4.2\,\text{V}$ and the maximum charging current should not be higher than

$I_{\text{Bat,1,cell}} = 7\,\text{A}$ [13]. In order to charge the battery as fast as possible either the maximum voltage or maximum current should be applied to the battery. The requested battery charging current, i.e. the output current of the boost converter i_{BC}, is therefore

$$i^*_{\text{BC}} = \begin{cases} i_{\text{Bat,max,cha}} & , i_{\text{Bat,max,cha}} < I_{\text{Bat,1,cell}} \\ I_{\text{Bat,1,cell}} & , i_{\text{Bat,max,cha}} \geq I_{\text{Bat,1,cell}} \end{cases} \quad [\text{A}], \tag{2.3}$$

which means that the requested output power of the boost converter is

$$p^*_{\text{BC}} = v_{\text{Bat}} i^*_{\text{BC}} \quad [\text{W}] \tag{2.4}$$

The requested charging current makes sure that neither the maximum allowed voltage or current are exceeded. However, for a big battery package the required charging power might be so high that a special charging station is necessary.

The requested input current of the boost converter, i.e. the rectifier current i_{FC}, can be calculated by Equation (F.8) and (2.4):

$$i^*_{\text{RF}} = \frac{-\left(V_{\text{th,BC}} - v_{\text{RF}}\right) - \sqrt{\left(V_{\text{th,BC}} - v_{\text{RF}}\right)^2 - 4R_{\text{BC}}p^*_{\text{BC}}}}{2R_{\text{BC}}} \quad [\text{A}] \tag{2.5}$$

The grid RMS-current can therefore from Equation (E.5) be calculated as

$$I_{\text{Grid}} = \begin{cases} \sqrt{\frac{2}{3}} i^*_{\text{RF}} & , \sqrt{\frac{2}{3}} i^*_{\text{RF}} < I_{\text{Grid,max}} \\ I_{\text{Grid,max}} & , \sqrt{\frac{2}{3}} i^*_{\text{RF}} \geq I_{\text{Grid,max}} \end{cases} \quad [\text{A}] \tag{2.6}$$

Thereby it is ensured that the maximum RMS grid current not is exceeded. The actual values can therefore be obtained by calculating backwards, i.e.

$$i_{\text{RF}} = \sqrt{\frac{3}{2}} I_{\text{Grid}} \quad [\text{A}] \tag{2.7}$$

$$p_{\text{RF}} = v_{\text{RF}} I_{\text{RF}} \quad [\text{W}] \tag{2.8}$$

$$p_{\text{BC}} = p_{\text{RF}} - R_{\text{BC}} I^2_{\text{RF}} - V_{\text{th,BC}} I_{\text{RF}} \quad [\text{W}] \tag{2.9}$$

$$I_{\text{BC}} = \frac{p_{\text{BC}}}{v_{\text{Bat}}} \quad [\text{A}] \tag{2.10}$$

In Figure 2.4 the battery state-of-charge, current, voltage, and the power of the grid and braking resistor can be seen. It is understood from Figure 2.4(a) that the battery is designed due to its power requirement and not the energy requirement as the state-of-charge has a minimum of approximately 0.4 which is higher than the minimum allowed value of $SoC_{\text{Bat,min}} = 0.2$. In Figure 2.4(b) the battery current is shown. It is seen that the regenerative current, i.e. negative current, becomes higher the more discharged the battery is. This is because of the braking resistor which ensures that the battery voltage not exceeds the maximum allowed value $V_{\text{Bus,max}}$. In Figure 2.4(c-d) it can be seen that the braking resistor dumps power when the maximum battery voltage is reached. In this figure the battery and grid power is also shown. It is seen that the charging of the battery is limited by the maximum allowed grid power $P_{\text{Grid,max}}$. After approximately two hours the battery reaches the maximum voltage, and it is therefore seen that the battery then is charged under constant-voltage approach, which means that the battery current and power and grid power slowly are decreased until the battery reaches its initial state-of-charge value.

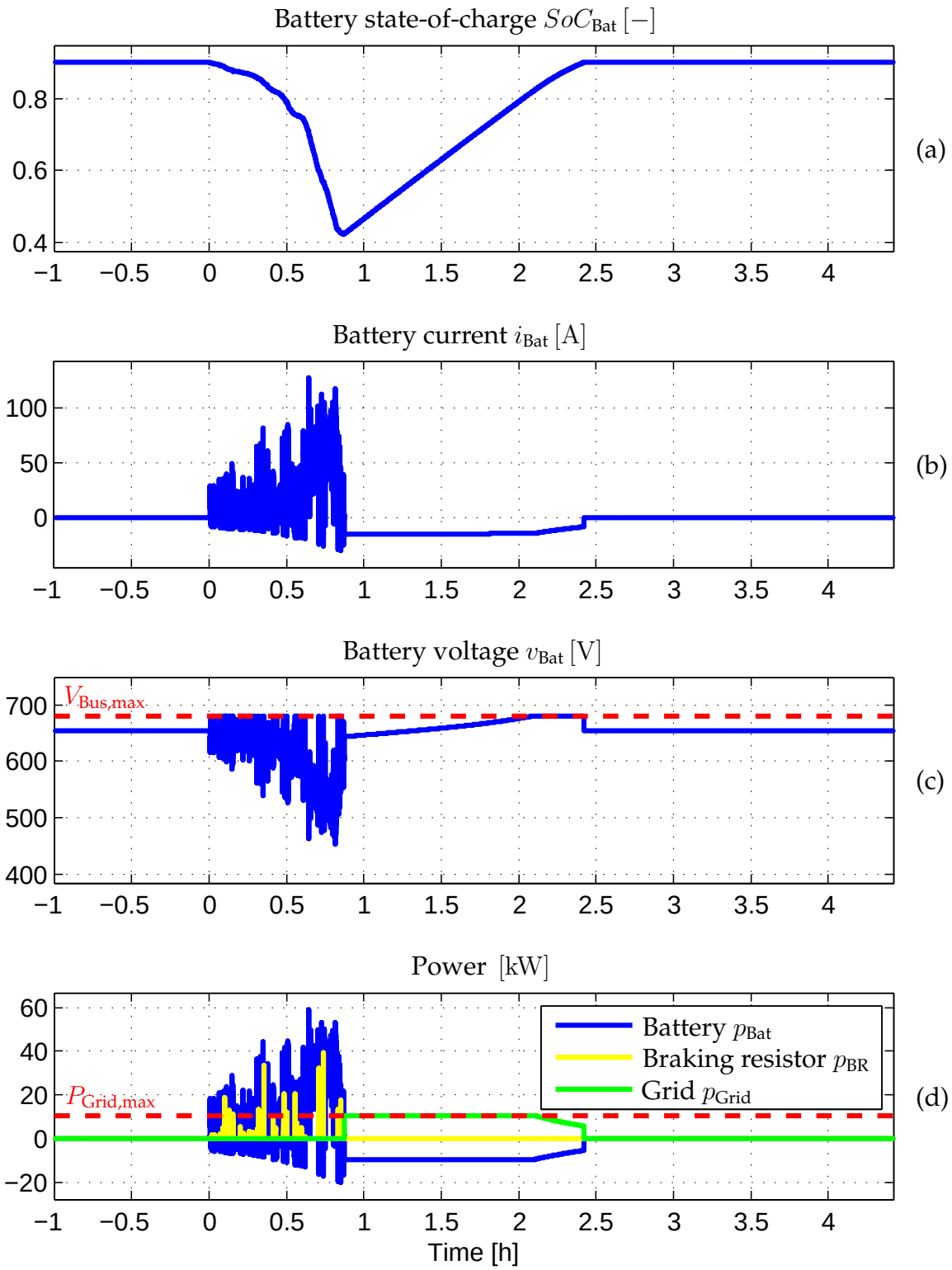

Figure 2.4: Simulation results of the BEV when it is designed for $50.9\,\text{km}$. (a) Battery state-of-charge. (b) Battery current. (c) Battery voltage. (d) Power of the Battery, grid, and braking resistor.

Sizing

Many types of batteries exist, but the Lithium Ion (LiIon) battery is considered to be the preferred choice for hybrid and pure electric vehicles in the short term and long term run. It is chosen to use the VL 37570 from Saft [13]. This battery is for mobile applications and has an energy density of $385\,\mathrm{Wh/L}$ and specific energy of $175\,\mathrm{Wh/kg}$. However, it is chosen as it contains the right specifications in order to be able to make a proper model. The battery is modeled in Appendix A.

The number of series connected battery cells $N_{\text{Bat,s}}$ can be calculated from the bus voltage specification and the nominal cell voltage $V_{\text{Bat,cell,nom}}$. It is chosen to have a nominal bus voltage of $V_{\text{Bus,nom}} = 600\,\mathrm{V}$. The required number of series connected cells is therefore

$$N_{\text{Bat,s}} = \frac{V_{\text{Bus,nom}}}{V_{\text{Bat,cell,nom}}} = \frac{600\,\mathrm{V}}{3.7\,\mathrm{V}} \approx 162\,\mathrm{cells} \tag{2.11}$$

This mans that the minimum and maximum bus voltage are

$$V_{\text{Bus,min}} = N_{\text{Bat,s}} V_{Bat,min,cell} = 162 \cdot 2.5\,\mathrm{V} = 405\,\mathrm{V} \tag{2.12}$$

$$V_{\text{Bus,max}} = N_{\text{Bat,s}} V_{Bat,max,cell} = 162 \cdot 4.2\,\mathrm{V} = 680\,\mathrm{V} \tag{2.13}$$

The number of parallel strings $N_{\text{Bat,p}}$ are calculated in an iterative process. The flow chart of the sizing procedure of the BEV can be seen in Figure 2.5. In the "Initialization"-process the base parameters are defined, e.g. wheel radius and nominal bus voltage, initial power ratings of each component of the BEV are given, and the base driving cycle is loaded into the workspace of Matlab. In the "Decide repetitions of the base driving cycle"-process it is specified how many times the base driving cycle should be repeated. The base driving cycle has a distance of $50.88\,\mathrm{km}$. If one wish to design a BEV that have range of e.g. $350\,\mathrm{km}$ the number of repetitions is $N_{\text{dc}} = \text{round}\left(\frac{350\,\mathrm{km}}{50.88\,\mathrm{km}}\right) = 7$. In the "Is the minimum number of parallel strings obtained?"-decision block is it verified if the minimum number of parallel strings that fulfills both the energy and power requirements of the battery have been reached. If not a "Simulation routine"-process is executed. This process are executed several times during the sizing procedure and its flow chart is therefore shown separately in Figure 2.5. This process consist of three sub-processes. The first sub-process is "Design components". In this process the parameters of each component of the BEV are determined, e.g. motor and power electronic parameters. The next sub-process is the "Vehicle simulation"-process. In this process the Simulink-model of the BEV is executed due to the parameters specified in the previous sub-process. In the third and last sub-process, i.e. the "Calculate the power and energy of each component"-process, the energy and power of each component of the BEV are calculated. The three sub-processes in the "Simulation routine"-process are executed three times in order to make sure that BEV parameters and energy and power of the BEV converges to the same values for the same input. After the "Simulation routine"-process is finish the "Calculate number of parallel strings"-process is applied. In this process the number of parallel strings $N_{\text{Bat,p}}$ is either increased or decreased. When the minimum

possible number of parallel strings that fulfills both the energy and power requirements of the battery have been found the "Simulation routine"-process is executed in order to calculate the grid energy due to the final number of parallel strings.

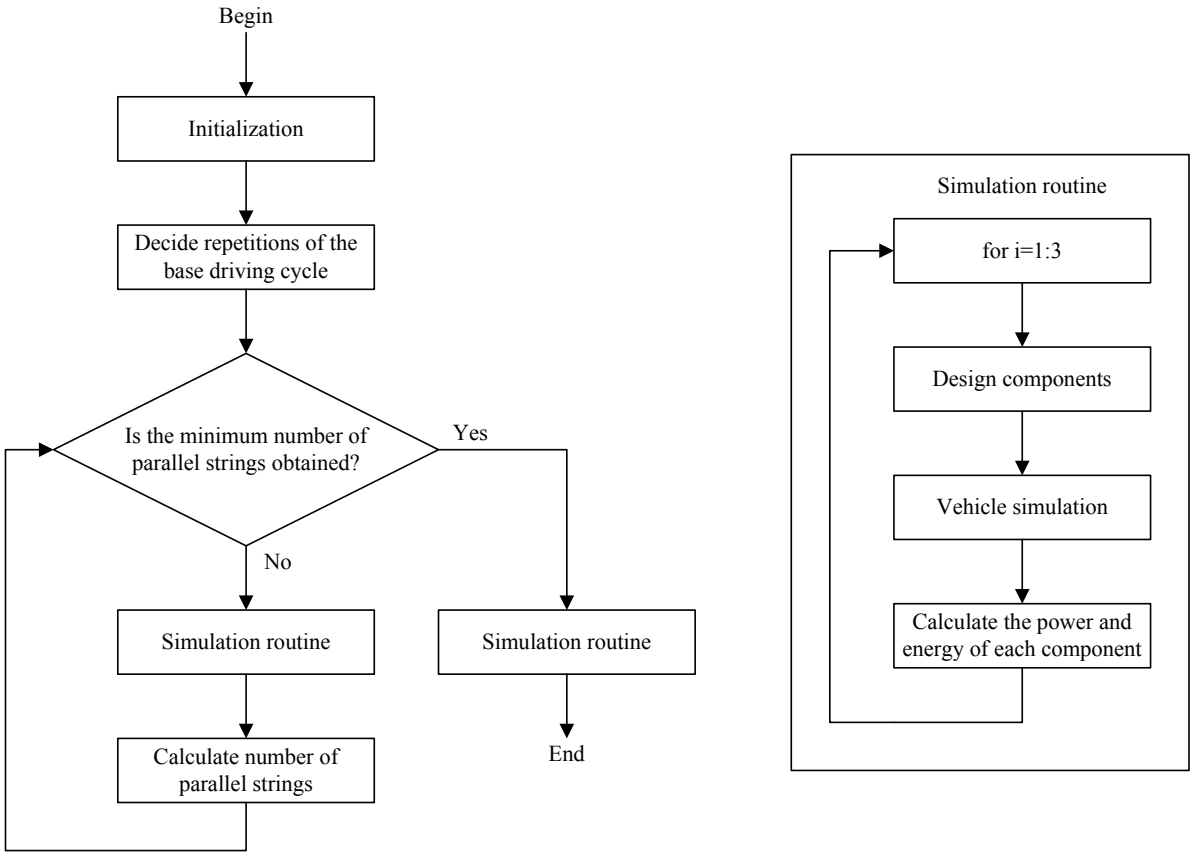

Figure 2.5: Sizing procedure of BEV.

In Figure 2.6 it can be seen how the "Calculate number of parallel strings"-process finds the minimum number of parallel strings $N_{\text{Bat,p}}$ that fulfills both the energy and power requirements. In Figure 2.6(a) the minimum state-of-charge min(SoC_{Bat}) is shown and in Figure 2.6(b) the maximum battery discharge current max($i_{\text{Bat,cell}}$) is shown. From the figure it is understood that the first iteration is for $N_{\text{Bat,p}} = 10$. However, both the minimum state-of-charge and maximum discharge current are satisfying their limits, i.e. $SoC_{\text{Bat,min}} = 0.2$ and $I_{\text{Bat,max,cell}} = 28\,\text{A}$, respectively. Therefore is the number of parallel strings reduced to $N_{Bat,p} = 3$ for iteration number two. However, now both the state-of-charge and maximum current requirements are exceeded and therefore the number of parallel strings is increased to $N_{\text{Bat,p}} = 8$ for iteration three. This process continuous until iteration number six where the number of parallel strings settles to $N_{\text{Bat,p}} = 6$, as this is the minimum number of parallel strings which ensures that both the state-of-charge and maximum current requirements are fulfilled.

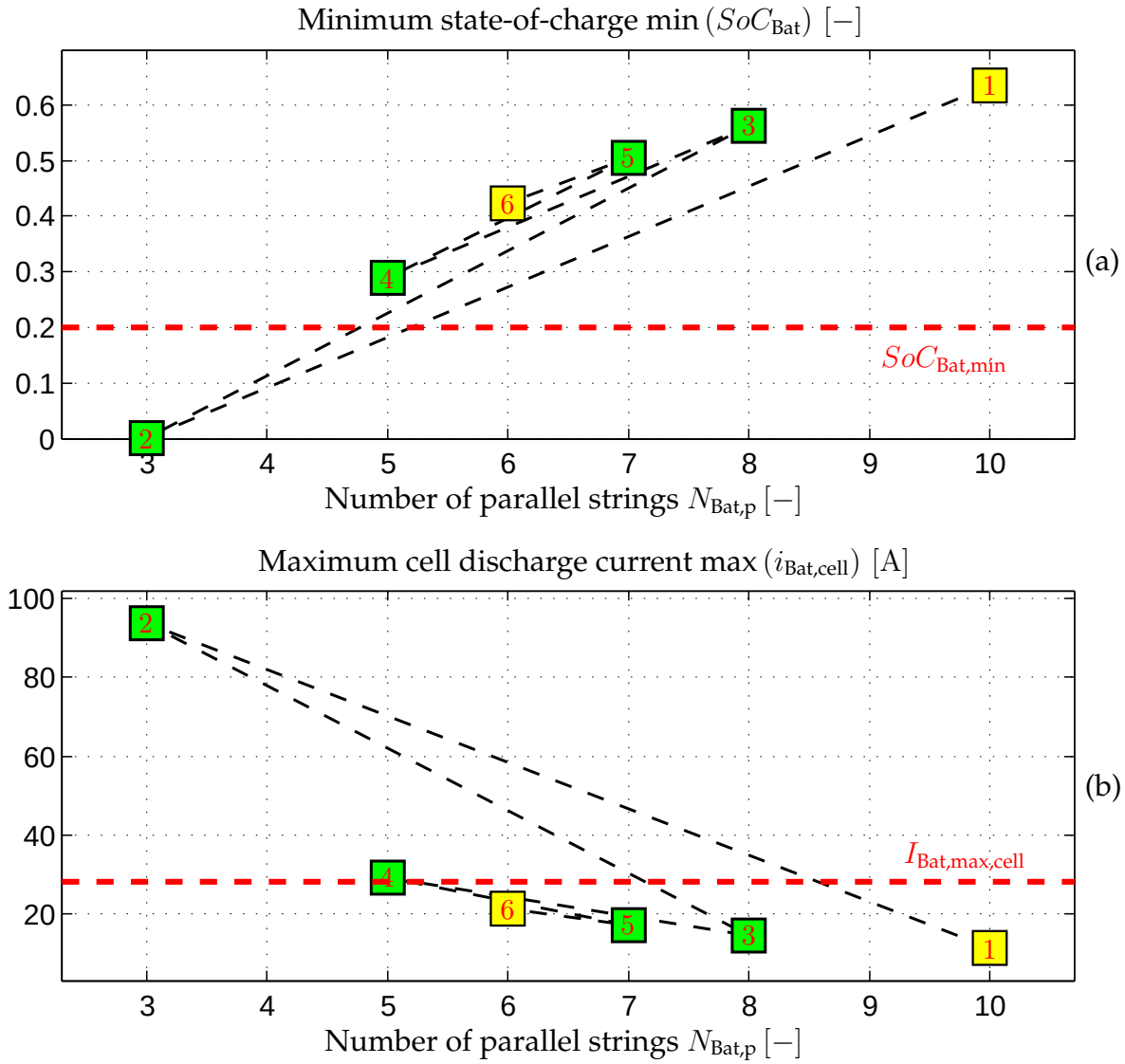

Figure 2.6: Number of parallel strings $N_{\text{Bat,p}}$ due to the "Calculate number of parallel strings"-process. The numbers in the green and yellow boxes indicate the iteration number of the design procedure. The yellow boxes are the first and last iteration number. (a) Minimum state-of-charge $SoC_{\text{Bat,min}}$. The red dashed horizontal lines indicates the minimum allowed state-of-charge. (b) Maximum cell discharge current max$(i_{\text{Bat,cell}})$. Dashed red horizontal line indicates the maximum allowed discharge current.

2.4 FUEL CELL HYBRID ELECTRIC VEHICLE

The components of the FCHEV can be seen in Figure 2.7. When comparing with the diagram of the BEV in Figure 2.2 on page 7 it is seen that from the boost converter to the wheels the two vehicles shares the same component. In the BEV a rectifier, which rectifies the grid voltage and current, is connected to the boost converter, but in the FCHEV a fuel cell is connected to the boost converter. The fuel cell is fed from a hydrogen tank.

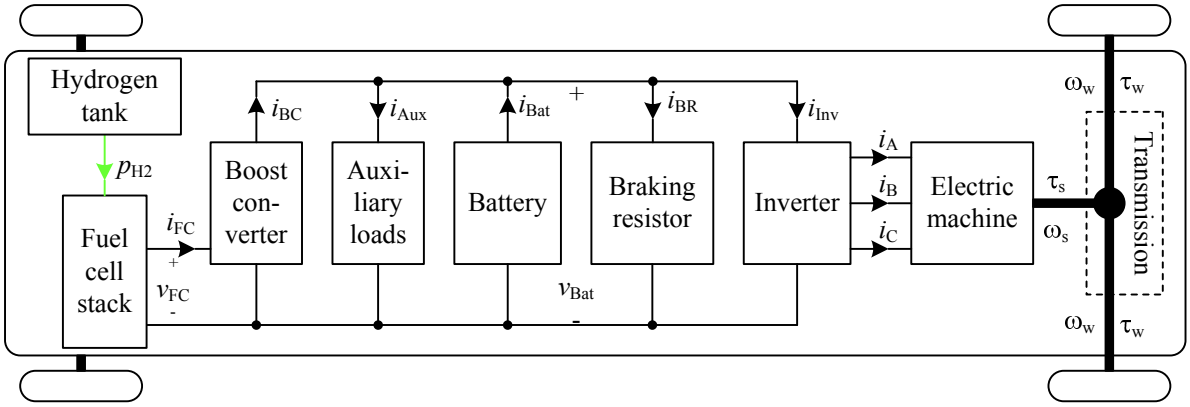

Figure 2.7: Main components of the FCHEV.

Fuel Cell

The sizing of the fuel cell is a trade off between efficiency, cost, and flexibility. The higher fuel cell power rating, the higher efficiency and cost. The disadvantages of the BEV is the long charging time of the batteries. In principle a fuel cell vehicle should not have this problem. However, if the vehicle should be able to run at maximum speed by the fuel cell alone, it would be quite expensive. Therefore the fuel cell is designed to provide the average power due to the driving cycle. The battery then provides the difference between the needed power and the fuel cell power. The chosen driving cycle (In Figure 1.1 on page 2) starts with city driving and finish with motorway driving. This means that the power consumption is higher in the end of the cycle than in the beginning. As the battery initial is charged to $SoC_{\text{Bat,Ini}} = 0.9$ the extra energy needed for the motorway driving cannot be stored in the battery during the city driving. Therefore the fuel cell needs to recharge the battery after the cycle is finish. This can also be seen in Figure 2.8 where the characteristics of a FCHEV designed for $508.8\,\text{km}$ are shown. The driving cycle then consist of a repetition of the original driving cycle 10 times. In Figure 2.8(a) it therefore seen that in the period with city driving (and therefore low power consumption) the battery is being charged. Due to the smaller battery package (in compare to the BEV) the battery cannot handle all the braking energy and a relative large amount of power is therefore dissipated in the braking resistor as shown in Figure 2.8(d). In Figure 2.8(d) it is also noticed that the negative traction power is bigger than the positive.

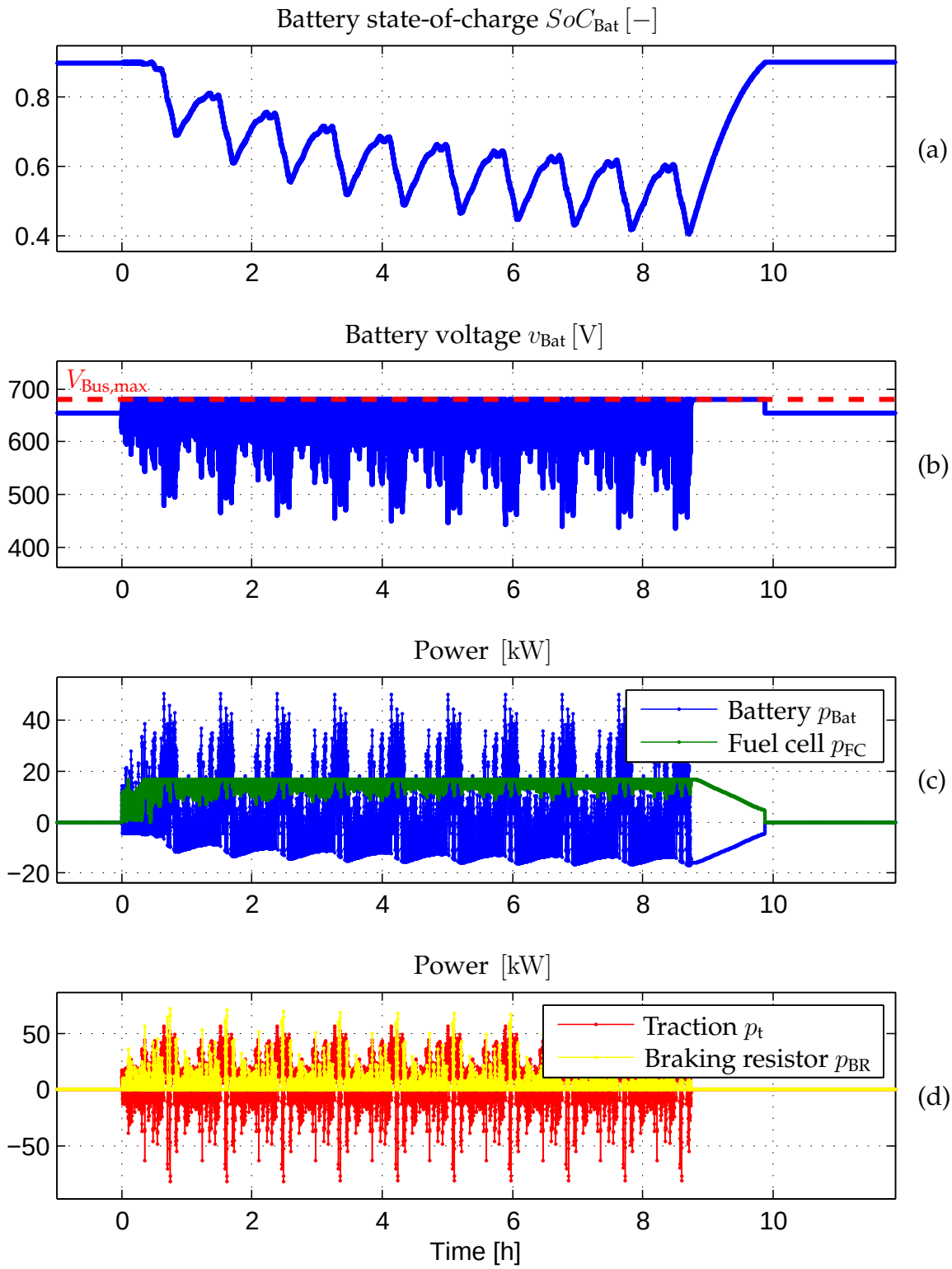

Figure 2.8: Simulation results of the FCHEV when it is designed for 508.8 km. (a) Battery state-of-charge. (b) Battery voltage. (c) Power of the battery and fuel cell. (d) Power due to the traction and braking resistor.

Simulation Model

The block diagram of the overall vehicle model can be seen in Figure 2.9. It is noticed that the structure is quite similar to simulink model of the BEV shown in Figure 2.3 on page 8.

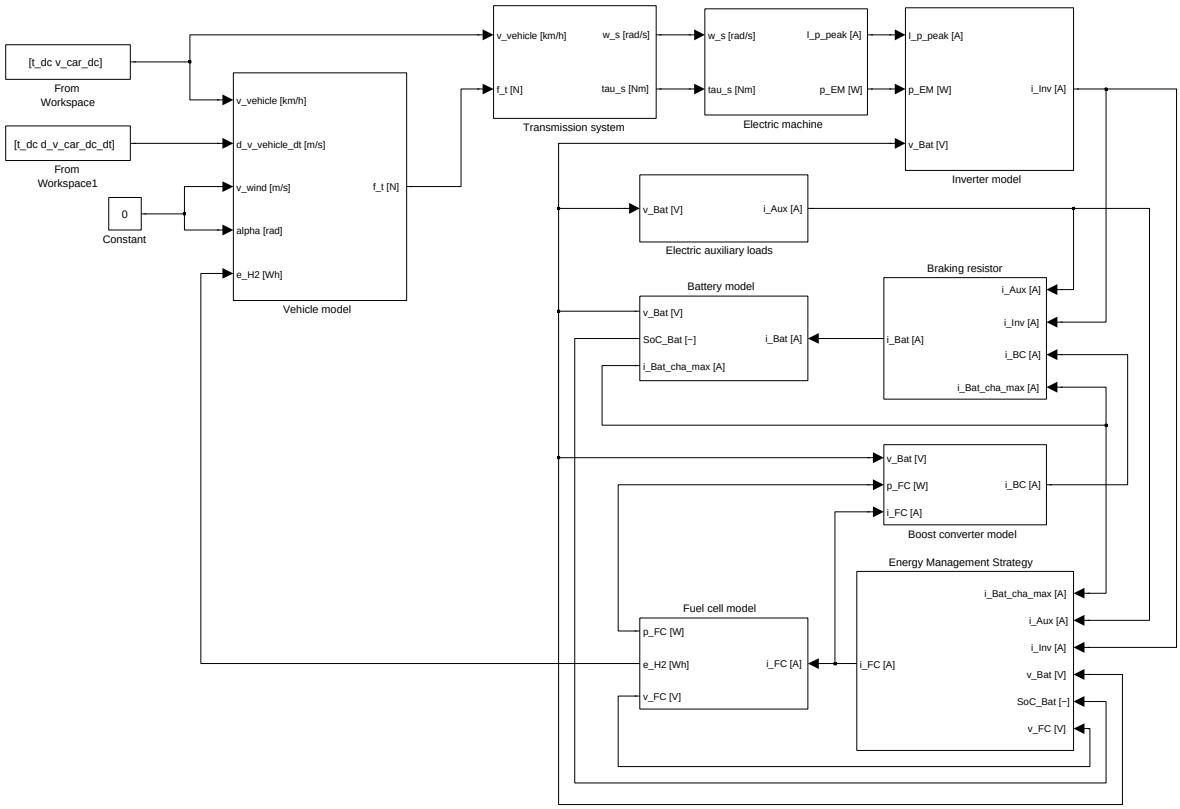

Figure 2.9: Simulink model of the overall FCHEV.

2.5 KEY FIGURES

The BEV and FCHEV will be assessed with respect to the total car mass and cost, tank-to-wheel efficiency, energy consumption per km, and volume of the power system.

Energy per km

The energy per km is calculated relative to the "tank"-energy. Therefore

$$E_{\text{tank}} = \begin{cases} E_{\text{Grid}} & \text{, BEV} \\ E_{\text{H2}} & \text{, FCHEV} \end{cases} \tag{2.14}$$

$$\frac{E_{\text{tank}}}{\text{km}} = \frac{E_{\text{tank}}}{\text{Distance}} \tag{2.15}$$

where	E_{tank}	$[\text{Wh}]$	Tank or input energy
	E_{Grid}	Wh	Energy delivered by the grid
	E_{H2}	$[\text{Wh}]$	Energy of the consumed hydrogen
	$\frac{E_{\text{tank}}}{\text{km}}$	$[\text{Wh/km}]$	Energy consumption per km
	Distance	$[\text{km}]$	Traveling distance

Efficiency

The vehicle efficiency is defined as the energy delivered to the contact surface between the road and driving wheels E_{t} relative to the tank energy, i.e.

$$\eta_{\text{TW}} = \frac{E_{\text{t}}}{E_{\text{tank}}} 100\,\% \tag{2.16}$$

where	η_{TW}	$[\%]$	Tank-to-wheel efficiency
	E_{t}	$[\text{Wh}]$	Traction energy

Total Mass

The car mass is given by

$$M_{\text{Car}} = \begin{cases} M_{\text{glider}} + M_{\text{person}} + M_{\text{EM}} + M_{\text{Inv}} \\ \quad + M_{\text{Bat}} + M_{\text{BC}} + M_{\text{BR}} + M_{\text{RF}} & \text{, BEV} \\ M_{\text{glider}} + M_{\text{person}} + M_{\text{EM}} + M_{\text{Inv}} \\ \quad + M_{\text{Bat}} + M_{\text{BC}} + M_{\text{BR}} + M_{\text{FC}} + M_{\text{H2}} + M_{\text{sto}} & \text{, FCHEV} \end{cases} \tag{2.17}$$

$$M_{\text{EM}} = \frac{P_{\text{s,max}}}{1000\text{SP}_{\text{EM}}} \tag{2.18}$$

$$M_{\text{Inv}} = \frac{P_{Inv,rat}}{1000\text{SP}_{Inv}} \tag{2.19}$$

$$M_{\text{Bat}} = M_{\text{Bat,cell}} N_{\text{Bat,s}} N_{\text{Bat,p}} \tag{2.20}$$

$$M_{\text{BC}} = \frac{P_{\text{BC,rat}}}{1000\text{SP}_{\text{Inv}}} \tag{2.21}$$

$$M_{\text{RF}} = \frac{P_{\text{RF,rat}}}{1000\text{SP}_{\text{Inv}}} \tag{2.22}$$

$$M_{\text{BR}} = \frac{P_{\text{BR,rat}}}{1000\text{SP}_{\text{Inv}}} \tag{2.23}$$

$$M_{\text{FC}} = M_{\text{FC,Cell}} N_{\text{FC,s}} N_{\text{FC,p}} \tag{2.24}$$

$$E_{\text{H2}} = \frac{1}{3600\,\text{s/h}} \int p_{\text{H2}} dt \tag{2.25}$$

$$M_{\text{H2}} = \frac{E_{\text{H2}} 3600\,\text{s/h}}{\text{LHV}_{\text{H2}}} \tag{2.26}$$

$$M_{\text{sto}} = \frac{E_{\text{H2}}}{1000\text{SE}_{\text{sto}}} \tag{2.27}$$

where	M_{Car}	$[\text{kg}]$	Total car mass
	M_{person}	$100\,\text{kg}$	Total person mass
	M_{EM}	$[\text{kg}]$	Mass of the electric machine
	M_{Inv}	$[\text{kg}]$	Inverter mass
	M_{Bat}	$[\text{kg}]$	Battery mass
	M_{BC}	$[\text{kg}]$	Mass of boost converter
	M_{RF}	$[\text{kg}]$	Mass of rectifier
	M_{BR}	$[\text{kg}]$	Mass of braking resistor
	M_{FC}	$[\text{kg}]$	Mass of fuel cell
	E_{H2}	$[\text{Wh}]$	Energy of consumed hydrogen
	M_{H2}	$[\text{kg}]$	Mass of hydrogen
	M_{sto}	$[\text{kg}]$	Mass of hydrogen storage

Volume of Power System

The volume of the power system of the two vehicles are given by

$$\text{Vol}_{\text{PS}} = \begin{cases} \text{Vol}_{\text{EM}} + \text{Vol}_{\text{Inv}} \\ \quad +\text{Vol}_{\text{Bat}} + \text{Vol}_{\text{BC}} + \text{Vol}_{\text{BR}} + \text{Vol}_{\text{RF}} & \text{, BEV} \\ \text{Vol}_{\text{EM}} + \text{Vol}_{\text{Inv}} \\ \quad +\text{Vol}_{\text{Bat}} + \text{Vol}_{\text{BC}} + \text{Vol}_{\text{BR}} + \text{Vol}_{\text{FC}} + \text{Vol}_{\text{H2}} + \text{Vol}_{\text{sto}} & \text{, FCHEV} \end{cases} \tag{2.28}$$

$$\text{Vol}_{\text{EM}} = \frac{P_{\text{s,max}}}{1000\text{PD}_{\text{EM}}} \tag{2.29}$$

$$\text{Vol}_{\text{Inv}} = \frac{P_{Inv,rat}}{1000\text{PD}_{Inv}} \tag{2.30}$$

$$\text{Vol}_{\text{Bat}} = \text{Vol}_{\text{Bat,cell}} N_{\text{Bat,s}} N_{\text{Bat,p}} \tag{2.31}$$

$$\text{Vol}_{\text{BC}} = \frac{P_{\text{BC,rat}}}{1000\text{PD}_{\text{Inv}}} \tag{2.32}$$

$$\text{Vol}_{\text{RF}} = \frac{P_{\text{RF,rat}}}{1000\text{PD}_{\text{Inv}}} \tag{2.33}$$

$$\text{Vol}_{\text{BR}} = \frac{P_{\text{BR,rat}}}{1000\text{PD}_{\text{Inv}}} \tag{2.34}$$

$$\text{Vol}_{\text{FC}} = \text{Vol}_{\text{FC,Cell}} N_{\text{FC,s}} N_{\text{FC,p}} \tag{2.35}$$

$$\text{Vol}_{\text{sto}} = \frac{E_{\text{H2}}}{1000\text{ED}_{\text{sto}}} \tag{2.36}$$

where	Vol_{Car}	[L]	Total car volume
	Vol_{EM}	[L]	Volume of the electric machine
	Vol_{Inv}	[L]	Inverter volume
	Vol_{Bat}	[L]	Battery volume
	Vol_{BC}	[L]	Volume of boost converter
	Vol_{RF}	[L]	Volume of rectifier
	Vol_{BR}	[L]	Volume of braking resistor
	Vol_{FC}	[L]	Volume of fuel cell
	Vol_{sto}	[L]	Volume of hydrogen storage

Total Cost

The cost of the vehicle is given by the sum of the individual component cost, i.e.

$$\text{Cost}_{\text{Car}} = \begin{cases} \text{Cost}_{\text{glider}} + \text{Cost}_{\text{EM}} + \text{Cost}_{\text{Inv}} + \text{Cost}_{\text{Bat}} \\ \quad + \text{Cost}_{\text{BC}} + \text{Cost}_{\text{BR}} + \text{Cost}_{\text{RF}} & \text{, BEV} \\ \text{Cost}_{\text{glider}} + \text{Cost}_{\text{EM}} + \text{Cost}_{\text{Inv}} + \text{Cost}_{\text{Bat}} \\ \quad + \text{Cost}_{\text{BC}} + \text{Cost}_{\text{BR}} + \text{Cost}_{\text{FC}} + \text{Cost}_{\text{sto}} & \text{, FCHEV} \end{cases} \tag{2.37}$$

$$\text{Cost}_{\text{EM}} = 16\frac{P_{\text{s,max}}}{1000} + 385 \text{ [14]} \tag{2.38}$$

$$\text{Cost}_{\text{Inv}} = \text{CP}_{\text{Inv}}\frac{P_{\text{Inv,rat}}}{1000} \tag{2.39}$$

$$\text{Cost}_{\text{BC}} = \text{CP}_{\text{Con}}\frac{P_{\text{BC,rat}}}{1000} \tag{2.40}$$

$$\text{Cost}_{\text{RF}} = \text{CP}_{\text{Inv}}\frac{P_{\text{RF,rat}}}{1000} \tag{2.41}$$

$$\text{Cost}_{\text{BR}} = \text{CP}_{\text{Inv}}\frac{P_{\text{BR,rat}}}{1000} \tag{2.42}$$

where	Cost_{Car}	[\$]	Total car cost
	$\text{Cost}_{\text{glider}}$	[\$]	Glider cost without power train. See Table 1.2.
	Cost_{EM}	[\$]	Cost of the electric machine
	Cost_{Inv}	[\$]	Inverter cost
	Cost_{Bat}	[\$]	Battery cost
	Cost_{BC}	[\$]	Cost of boost converter
	Cost_{RF}	[\$]	Cost of rectifier
	Cost_{BR}	[\$]	Cost of braking resistor
	CP_{Inv}	5 \$/kW	Inverter cost per kW power
	CP_{Con}	75 \$/kW	Converter cost per kW power

The cost parameters of the power electronics are based on U.S. Department of Energy's 2010 targets with a production of 100,000 per year [19].

2.6 SIMULATION RESULTS

Tank energy per km, tank-to-wheel efficiency, total vehicle mass and cost, and volume of power system are shown in Table 2.2 for the BEV and FCHEV. The key figures

are presented for different traveling distances. First of all it is noticed that the tank energy per km for the BEV is approximately half of the value for the FCHEV, and that the tank-to-wheel efficiency of the BEV is approximately double of the efficiency of the FCHEV. The is due to the higher efficiency of batteries than fuel cells. For both the BEV and FCHEV the tank energy per km becomes higher the longer distance. This is not surprising as the total car mass becomes higher when the required traveling distance increases. However, it is also noticed that the car mass of the BEV almost doubles when the vehicle is designed for $508.8\,\mathrm{km}$ instead of for $50.9\,\mathrm{km}$. For the FCHEV the increase in total car mass is much less significant. This is because the hydrogen storage specific energy ($2\,\mathrm{kWh/kg}$) is significant higher than for the battery ($\approx 0.274\,\mathrm{kWh/kg}$). The tank-to-wheel efficiency of the BEV increases by approximately $10\,\%$ when the vehicle is designed for $508.8\,\mathrm{km}$ instead of for $50.9\,\mathrm{km}$. This is because of the nature of the chosen battery. For short traveling distances the battery is designed to handle the peak powers for accelerations and not the energy. For the long traveling distances the battery is designed to provide enough energy for the trip and the battery can therefore easily handle the peak powers. Due to Peukert phenomenon is the efficiency of the battery higher the lower current as it also is seen in Table A.3 on page 42. In Figure 2.10 the relative energy of a given component relative to the tank or input energy is shown. The figure illustrates the two extreme cases, i.e. when the vehicle is designed for (a): $50.88\,\mathrm{km}$ and (b) $508.8\,\mathrm{km}$. The energy loss of the electric machines is $10\,\%$ and $13\,\%$ for the two cases. However, it most be emphases that except from the traction energy E_{t}, are the percentages in Figure 2.10 not efficiencies, but energy levels relative to the grid energy E_{Grid}.

The efficiency of the FCHEV does not change as significant as for the BEV. The relative energy consumption of the components of the FCHEV for the two extremes can be seen in Figure 2.11. It is seen that most of the energy is lost in the fuel cell. Therefore the relative energy of the other components (except of the energy dissipated in the braking resistor) are also smaller than in the cases of the BEV. Due to the fuel cell is the battery package of the FCHEV much smaller than for the BEV. This means that the battery cannot accept all the braking energy, and it is therefore led to the braking resistor instead of.

The volume of the power systems of cause increases when the traveling distance also increases. However, due to the higher energy density of hydrogen storage than of batteries the volume of the power system of the BEV increases more than for the FCHEV when the traveling distance increases. This higher increase is also seen in the total car cost. The cost of the FCHEV only increases by $26\,\%$ when the vehicle is designed for $508.8\,\mathrm{km}$ than for $50.88\,\mathrm{km}$, but the cost of the BEV more than triples. The BEV is cheaper for short traveling distances but becomes very expensive for long distances. However, it most be mentioned that the cost calculation only should be used as a qualified guess as there is a lot of uncertainty included in the cost calculation.

Based on the results in Table 2.2 two conclusion can be made of the BEV and FCHEV: The BEV energy consumption (both absolute and relative) of the BEV is significant better than for the FCHEV for both short and long traveling distances. In terms of total car mass, power system volume, and total car cost is the BEV "better" for short design distances. For design distances higher than $152.6\,\mathrm{km}$, $356.1\,\mathrm{km}$, and

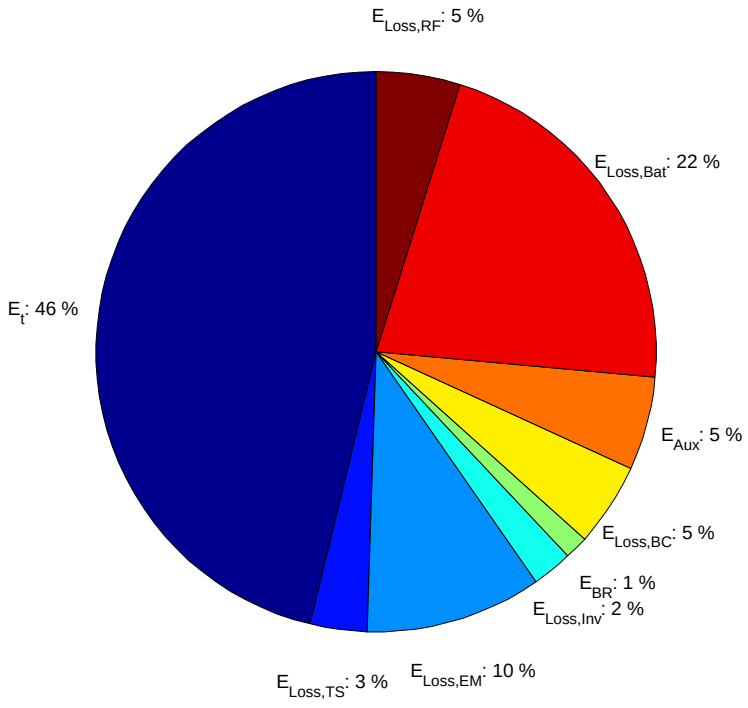

(a)

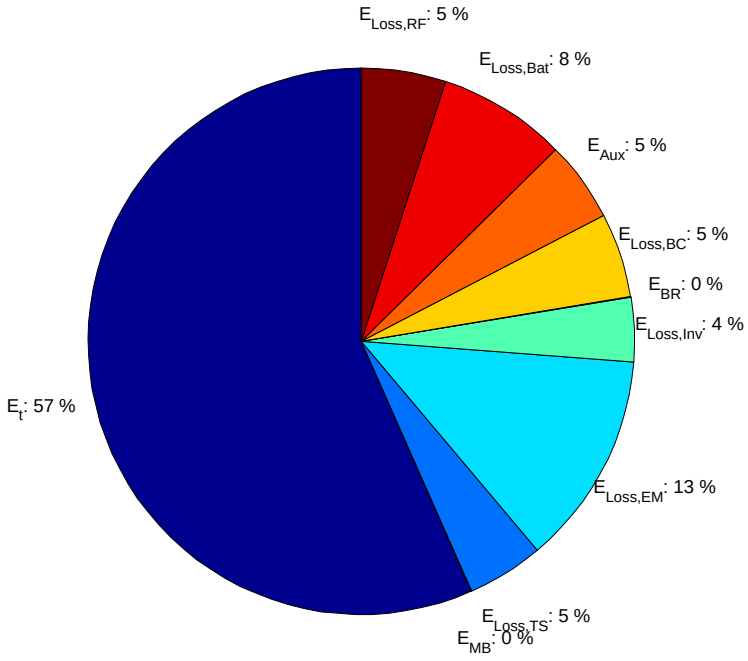

(b)

Figure 2.10: Energy pie of the BEV designed for (a) $50.9\,\mathrm{km}$ and (b) $508.8\,\mathrm{km}$. The percentage specifies the energy of a given component relative to the grid energy E_{Grid}. E_{t}: Traction energy. E_{MB}: Energy dissipated in the mechanical brakes. $E_{\mathrm{Loss,TS}}$: Loss of the transmission system. $E_{\mathrm{Loss,EM}}$: Loss of the electric machine. E_{Inv}: Inverter loss. E_{BR}: Energy dissipated in the braking resistor. $E_{\mathrm{Loss,BC}}$: Boost converter loss. E_{Aux}: Energy consumed by auxiliary devices. $E_{\mathrm{Loss,Bat}}$: Energy loss of the battery. $E_{\mathrm{Loss,RF}}$: Energy loss of the rectifier.

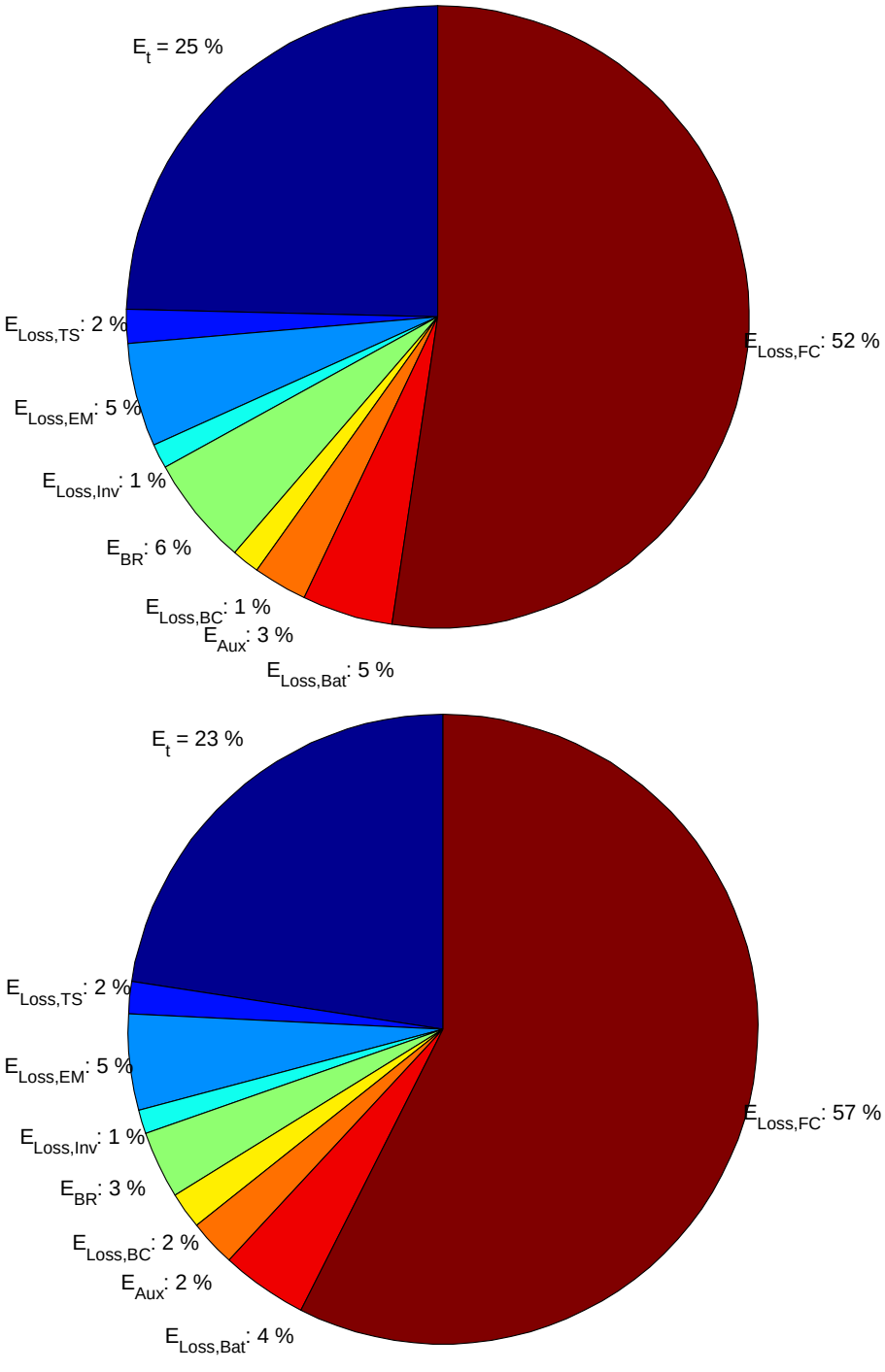

Figure 2.11: Energy pie of the FCHEV designed for (a) $50.88\,\mathrm{km}$ and (b) $508.8\,\mathrm{km}$. The percentage specifies the energy of a given component relative to the energy of the consumed hydrogen E_{H2}. E_{t}: Traction energy. E_{MB}: Energy dissipated in the mechanical brakes. $E_{\mathrm{Loss,TS}}$: Loss of the transmission system. $E_{\mathrm{Loss,EM}}$: Loss of the electric machine. E_{Inv}: Inverter loss. E_{BR}: Energy dissipated in the braking resistor. $E_{\mathrm{Loss,BC}}$: Boost converter loss. E_{Aux}: Energy consumed by auxiliary devices. $E_{\mathrm{Loss,Bat}}$: Energy loss of the battery. $E_{\mathrm{Loss,FC}}$: Fuel cell energy loss.

$203.5\,\mathrm{km}$ for the mass, volume, and cost, respectively, the FCHEV is a better choice. However, it should be mentioned that values for the FCHEV easily can be changed by increasing the fuel cell power rating, e.g. increasing the fuel cell power rating will probably have a negative effect on the cost, but a positive effect on the total car mass and power system volume.

	Designed traveling distance [km]										
	50.9	101.8	152.6	203.5	254.4	305.3	356.1	407.0	457.9	508.8	
Tank energy per km $\frac{E_{\text{Tank}}}{\text{km}}$ [Wh/km]	305.2	290.1	281.1	283.0	289.4	296.0	306.7	316.2	328.5	344.6	BEV
	583.6	601.4	616.7	621.7	631.8	641.4	650.8	660.1	669.8	679.6	FCHEV
Tank-to-wheel Efficiency η_{TW} [%]	46.2	49.5	52.9	54.3	55.2	55.7	56.2	56.5	56.6	56.6	BEV
	24.6	24.0	23.6	23.7	23.5	23.3	23.1	22.9	22.7	22.6	FCHEV
Total car mass M_{car} [kg]	1,226	1,274	1,372	1,469	1,592	1,690	1,837	1,959	2,108	2,284	BEV
	1,274	1,292	1,310	1,351	1,369	1,388	1,408	1,428	1,449	1,470	FCHEV
Volume of power system Vol_{PS} [L]	98.8	120.1	162.6	205.5	259.2	302.2	366.8	420.8	486.0	563.3	BEV
	192.9	214.5	237.0	268.4	291.5	315.2	339.5	364.5	390.2	416.8	FCHEV
Total car cost Cost_{car} [USD]	22,751	24,863	29,075	33,307	38,606	42,850	49,217	54,529	60,942	68,513	BEV
	30,138	30,834	31,556	33,246	33,983	34,738	35,515	36,313	37,135	37,983	FCHEV

Table 2.2: Tank energy per km, tank-to-wheel efficiency, total vehicle mass and cost, and volume of power system. The key figures are shown for different traveling distances.

3 Conclusion

A simulation model of a Battery Electric Vehicle (BEV) and a Fuel Cell Hybrid Electric Vehicle (FCHEV) have been developed in Matlab/simulink. The BEV is being powered by lithium batteries, and the FCHEV is supplied by a combination of lithium batteries and a proton exchange membrane fuel cell. The vehicles are first designed for a specific driving cycle, i.e. the electric machine, power electronic, battery, fuel cell, etc. are sized in order to handle the required power and energy. The driving cycle consist of three different environments, i.e. urban driving, road driving, and motorway driving. When the components have been sized the simulation program executes a simulation where the consumed energy is calculated. The simulation program also calculates the total vehicle mass and cost, volume of the power system. The driving cycle has a length of $50.9\,\mathrm{km}$, but it can be repeated several times in order to perform a longer traveling distance. Thereby the two vehicles can be compared in terms of mass, volume, cost, energy consumption, and efficiency for different traveling distances. The two vehicles have been compared for traveling distances between $50.9\,\mathrm{km}$ to $508.8\,\mathrm{km}$. For all the traveling distances the energy consumption per km and efficiency are significant better for the BEV than for the FCHEV. The average energy consumption per km is $304.1\,\mathrm{Wh/km}$ and $635.7\,\mathrm{Wh/km}$ for the BEV and FCHEV, respectively. The average tank-to-wheel efficiency of the BEV and FCHEV are $54.0\,\%$ and $23.4\,\%$, respectively. For the energy per km and efficiency the input energy is the grid energy for the BEV and energy of the hydrogen for the FCHEV. For both vehicles the battery is recharged to the initial state-of-charge. For the total car mass and cost and volume of the power system, the results are two-sided. For short distance the BEV is lighter, has smaller volume of the power system, and are cheaper than the FCHEV. However, when the traveling distance increases the difference becomes smaller, and at long distances the FCHEV are the lightest, smallest, and cheapest.

As a final remark it most be mentioned that the cost modeling included in the simulation models are relative simple and should therefore only be used as a "qualified guess". It should also be mentioned that the modeling are based on data sheet specifications or theoretically considerations. The different models have therefore not been verified by laboratory experiments, which is recommendable for future work. The two vehicles have been designed in order to satisfy the power end energy requirement. However, in order to increase the efficiency the components can be rated higher than necessary, but this will also increase the cost of the system. If better cost models are used a better compromise between efficiency and cost can be made. For small distance the battery is sized due to its power requirement, and for long distance

it is rated due to its energy requirement. Therefore, in order to improve the efficiency for the same (or close to) cost, different batteries with different power-energy characteristics could also be included in the design process.

Bibliography

[1] Datasheet of ballard fcgen-1020acs fuel cell stack, October 2010. http://www.ballard.com/files/pdf/Spec_Sheets/FCgen-1020ACS_with_csa.pdf.

[2] Analysis of power balancing with fuel cells & hydrogen priduction plans in denmark, March 2009. CanDan 1.5 project report.

[3] F. Casanellas. Losses in pwm inverters using igbts. *IEE Proceedings - Electric Power Applications*, 141(5):235 – 239, September 1994.

[4] De danske bilimportører, 2010. http://www.bilimp.dk/statistics/index.asp.

[5] Mehrdad Ehsani, Yimin Gao, Sebastien E. Gay, and Ali Emadi. *Modern Electric, Hybrid Electric, and Fuel Cell Vehicles - Fundamentals, Theory, and Design*. CRC Press LLC, first edition, 2005. ISBN 0-8493-3154-4.

[6] Ali Emadi. *Handbook of Automotive Power Electronics and Motor Drives*. Taylor & Francis, first edition, 2005. ISBN 0-8247-2361-9.

[7] Iea energy technology essentials - fuel cells, April 2007. http://www.iea.org/techno/essentials6.pdf.

[8] Kasper Køtter Jensen, Kasper Aastrup Mortensen, Kenneth Jessen, Tommy Frandsen, Gunner Runólfsson, and Thorunn Thorsdóttir. Design of spmsm drive system for renault kangoo. *Report - Group 43-A - EMSD8*, May 2009.

[9] S.M. Lukic and A. Emadi. Performance analysis of automotive power systems: effects of power electronic intensive loads and electrically-assisted propulsion systems. *Proc. of IEEE Vehicular Technology Conference (VTC)*, 3:1835 – 1839, 2002.

[10] Tony Markel, Matthew Zolot, Keith B. Wipke, and Ahmad A. Pesaran. Energy storage system requirements for hybrid fuel cell vehicles. *Proc. of Advanced Automotive Battery Conference*, June 2003.

[11] Ned Mohan, Tore M. Underland, and William P. Robbins. *Power electronics*. John Wiley, third edition, 2003. ISBN 0-471-22693-9.

[12] Mitch Olszewski. Evaluation of the 2007 toyota camry hybrid synergy drive system. *U.S. Department of Energy*, April 2008.

[13] Saft, 2010. http://www.saftbatteries.com.

[14] A. Simpson. Cost-benefit analysis of plug-in hybrid electric vehicle technology. *Proc. of International Battery, Hybrid and Fuel Cell Electric Vehicle Symposium and Exhibition (EVS-22)*, October 2006.

[15] Skatteministeriet, registreringsafgift, 2010. `http://www.skm.dk/tal_statistik/satser_og_beloeb/228.html`.

[16] Tire code, wikipedia, 2010. `http://da.wikipedia.org/wiki/D%C3%A6k_(hjul)`.

[17] Toyota avensis, specifications, 2010. `http://www.toyota.dk/cars/new_cars/avensis/fullspecs.aspx`.

[18] Uqm technologies, 2010. `http://www.uqm.com`.

[19] Edward J. Wall. Plug-in hybrid electric vehicle r&d plan - external draft, February 2007.

A Battery

In this appendix a battery will be modeled. The parameters will be extracted from data sheet specifications.

A.1 Specifications and Characteristics

The specifications of a single base cell can be seen in Table A.1.

Manufacture	Saft
Type	VL 37570
Maximum voltage $V_{\text{Bat,max,cell}}$	$4.2\,\text{V}$
Nominal voltage $V_{\text{Bat,nom,cell}}$	$3.7\,\text{V}$
Minimum voltage $V_{\text{Bat,min,cell}}$	$2.5\,\text{V}$
$1\,\text{h}$ capacity $Q_{\text{1,cell}}$	$7\,\text{Ah}$
Nominal $1\,\text{h}$ discharge current $I_{\text{Bat,1,cell}}$	$7\,\text{A}$
Maximum pulse discharge current $I_{\text{Bat,max,cell}}$	$28\,\text{A}$
Mass $M_{\text{Bat,cell}}$	$0.149\,\text{kg}$
Volume $\text{Vol}_{\text{Bat,cell}}$	$0.0654\,\text{L}$
Cost CE_{Bat} [2]	$250\,\$/\text{kWh}$

Table A.1: Data sheet specifications of Saft VL 37570 LiIon battery [13] and cost estimation.

In Figure A.1 the capacity with different discharge currents can be seen. Almost no difference in capacity is seen for current below or close to the nominal discharge current at $1C$. However, the double nominal current $2C$ reduces the capacity significant.

In Figure A.2 the voltage, current, and state-of-charge of the battery is shown for different constant charging currents. The charging current is constant until the terminal voltage becomes equal to $4.2\,\text{V}$. Thereafter the current decreases as the voltage is kept at $4.2\,\text{V}$. When the current becomes equal to zero, the battery is fully charged, i.e. the state-of-charge is equal to 1.

A.2 Modeling

The battery will only be modeled in steady-state, i.e. the dynamic behavior is not considered. The electric equivalent circuit diagram can be seen in FigureA.3. The

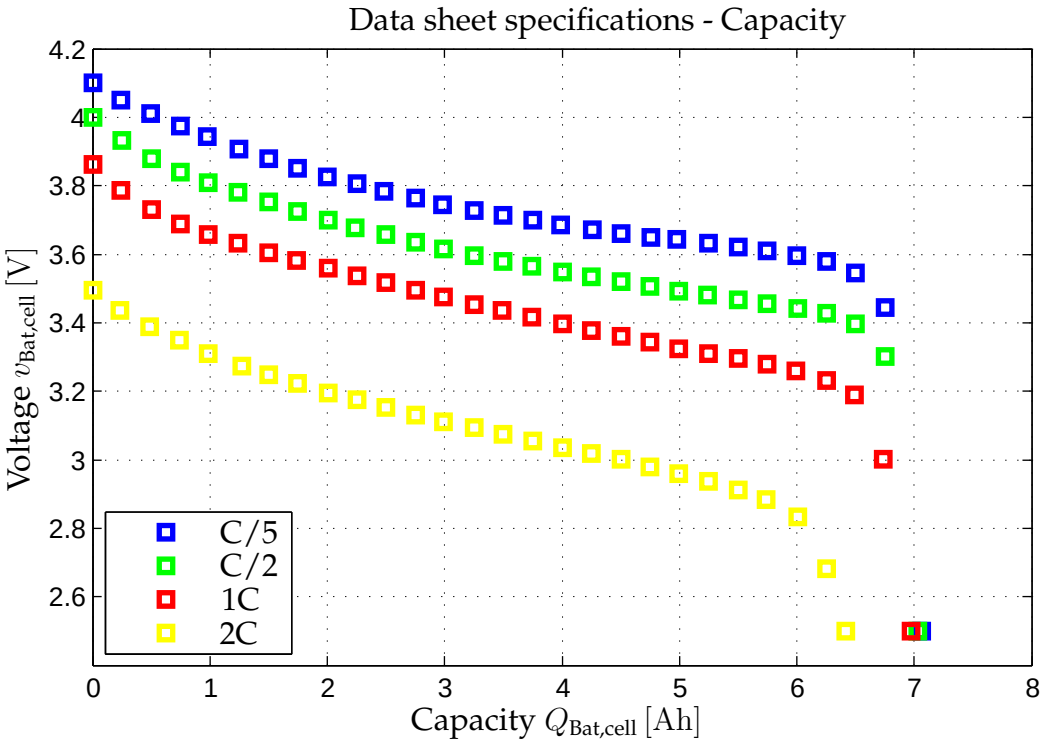

Figure A.1: Capacity for different constant discharge currents according to the data sheet.

battery model consist of an internal voltage source $v_{\text{Bat,int,cell}}$ and two inner resistances $R_{\text{Bat,cha,cell}}$ used for charging and $R_{\text{Bat,dis,cell}}$ for discharging. The two diodes are ideal and have only symbolics meaning, i.e. to be able switch between the charging and discharging resistances. Discharging currents are treated as positive currents, i.e. charging currents are then negative.

Capacity

In Figure A.1 the capacity can be seen for different discharging currents. For current higher than the nominal the capacity is reduced. The phenomena can be modeled by the Peukert equation:

$$Q_{1\text{A}} = I_{\text{Bat,cell}}^{k} T_{\text{Bat}} \qquad [\text{Ah}] \tag{A.1}$$

where	$Q_{1\text{A}}$	[Ah]	Capacity for a discharge current of $I_{\text{Bat,cell}} = 1\,\text{A}$.
	k	[−]	Peukert number.
	T_{Bat}	[h]	Discharge time

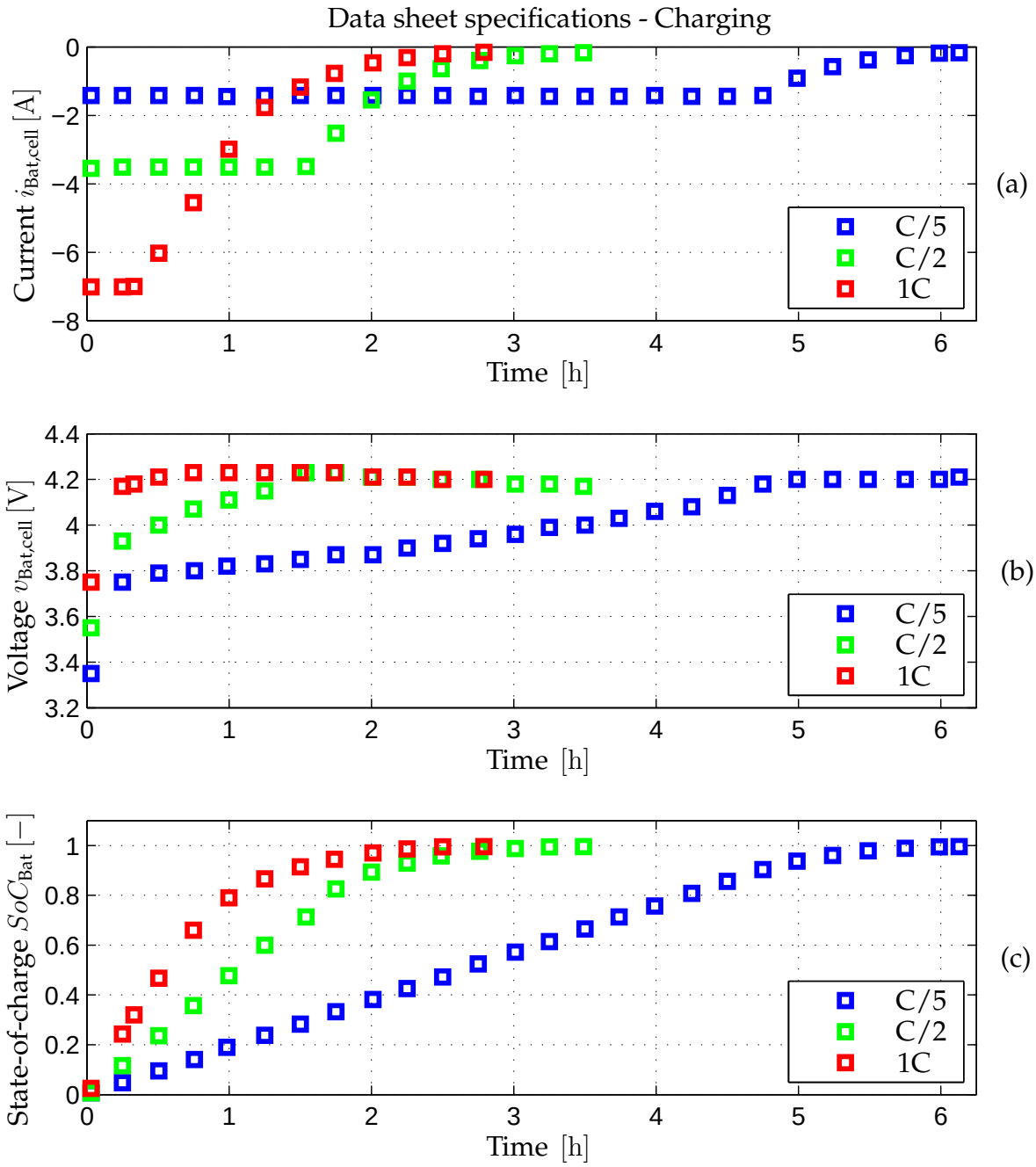

Figure A.2: Characteristics for different constant charging currents according to the data sheet. (a) Current. (b) Voltage. (c) State-of-charge.

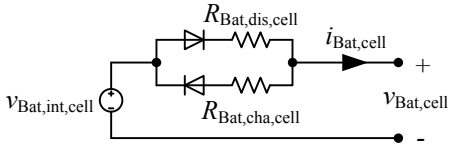

Figure A.3: Electric equivalent circuit of battery.

By manipulating Equation A.1 the Peukert number is given by

$$Q_{1A} = I_{\text{Bat,cell}}^{k} T_{\text{Bat}} = I_{\text{Bat,1,cell}}^{k} T_{\text{Bat,1}} \quad [\text{Ah}] \tag{A.2}$$

$$\Updownarrow$$

$$I_{\text{Bat,cell}}^{k-1} \underbrace{I_{\text{Bat,cell}} T_{\text{Bat}}}_{Q_{\text{Bat,cell}}} = I_{\text{Bat,1,cell}}^{k-1} \underbrace{I_{\text{Bat,1,cell}} T_{\text{Bat,1}}}_{A_{\text{Bat,1,cell}}} \quad [\text{Ah}] \tag{A.3}$$

$$\Updownarrow$$

$$k = \frac{\log\left(Q_{\text{Bat,cell}}\right) - \log\left(Q_{\text{Bat,1,cell}}\right)}{\log\left(I_{\text{Bat,1,cell}}\right) - \log\left(I_{\text{Bat,cell}}\right)} + 1 \quad [-] \tag{A.4}$$

When applying Equation A.4 to the data sheet capacities in Figure A.1 the results in Table A.2 are obtained.

$I_{\text{Bat,cell}}\,[\text{A}]$	1.4	3.5	14.0
$k\,[-]$	1.0053	1.0062	1.1248

Table A.2: Calculation of the Peukert number.

The calculation of the Peukert number for the two low current levels in Table A.2 supports the curves in Figure A.1, i.e. no significant difference in capacity is seen for currents below the nominal discharge current, where the Peukert number is equal to one in these situations. The Peukert number is therefore current depending:

$$k = \begin{cases} 1 & I_{\text{Bat,cell}} \leq I_{\text{Bat,1,cell}} \\ 1.125 & I_{\text{Bat,cell}} > I_{\text{Bat,1,cell}} \end{cases} \quad [-] \tag{A.5}$$

From Equation A.2 the time a current $I_{\text{Bat,cell}}$ can be drawn is

$$T_{\text{Bat}} = \left(\frac{I_{\text{Bat,1,cell}}}{I_{\text{Bat,cell}}}\right)^{k} T_{\text{Bat,1}} \quad [\text{h}] \tag{A.6}$$

If a discharging current $I_{\text{Bat,cell}}$ is drawn for T_{Bat} hours until the minimum battery voltage $V_{\text{Bat,min,cell}} = 2.5\,\text{V}$ is reached, a charge of $Q_{\text{Bat,1,cell}}$ actual have "left" the battery. Seen from the battery side an equivalent discharge current $I_{\text{Bat,eq,cell}}$ have therefore been drawn for T_{Bat} hours. This equivalent discharge current $I_{\text{Bat,eq,dis}}$ is from Equation A.6 given by

$$Q_{\text{Bat,1,cell}} = I_{\text{Bat,1,cell}} T_{\text{Bat,1}} = I_{\text{Bat,eq,dis}} T_{\text{Bat}} \tag{A.7}$$

$$= I_{\text{Bat,eq,dis}} \left(\frac{I_{\text{Bat,1,cell}}}{I_{\text{Bat,cell}}}\right)^{k} T_{\text{Bat,1}} \quad [\text{Ah}] \tag{A.8}$$

$$\Updownarrow$$

$$I_{\text{Bat,eq,dis}} = I_{\text{Bat,1,cell}} \left(\frac{I_{\text{Bat,cell}}}{I_{\text{Bat,1,cell}}}\right)^{k} \quad [\text{A}] \tag{A.9}$$

Inner Resistance

The internal voltage source depends on the temperature and state-of-charge SoC_{Bat}. However, for simplicity only the state-of-charge is considered. The state-of-charge can be expressed by the depth-of-discharge DoD_{Bat}, i.e.

$$SoC_{\text{Bat}} = 1 - DoD_{\text{Bat}} \qquad [-] \tag{A.10}$$

The depth-of-discharge is defined relatively to the $1\,\text{h}$ capacity, i.e. $Q_{\text{Bat,1,cell}}$. Therefore

$$DoD_{\text{Bat}} = \int \frac{I_{\text{Bat,eq,dis}}}{Q_{\text{Bat,1,cell}}} dt \qquad [-] \tag{A.11}$$

$$\tag{A.12}$$

In Figure A.4 the battery voltage versus the depth-of-discharge for different discharge currents can be seen.

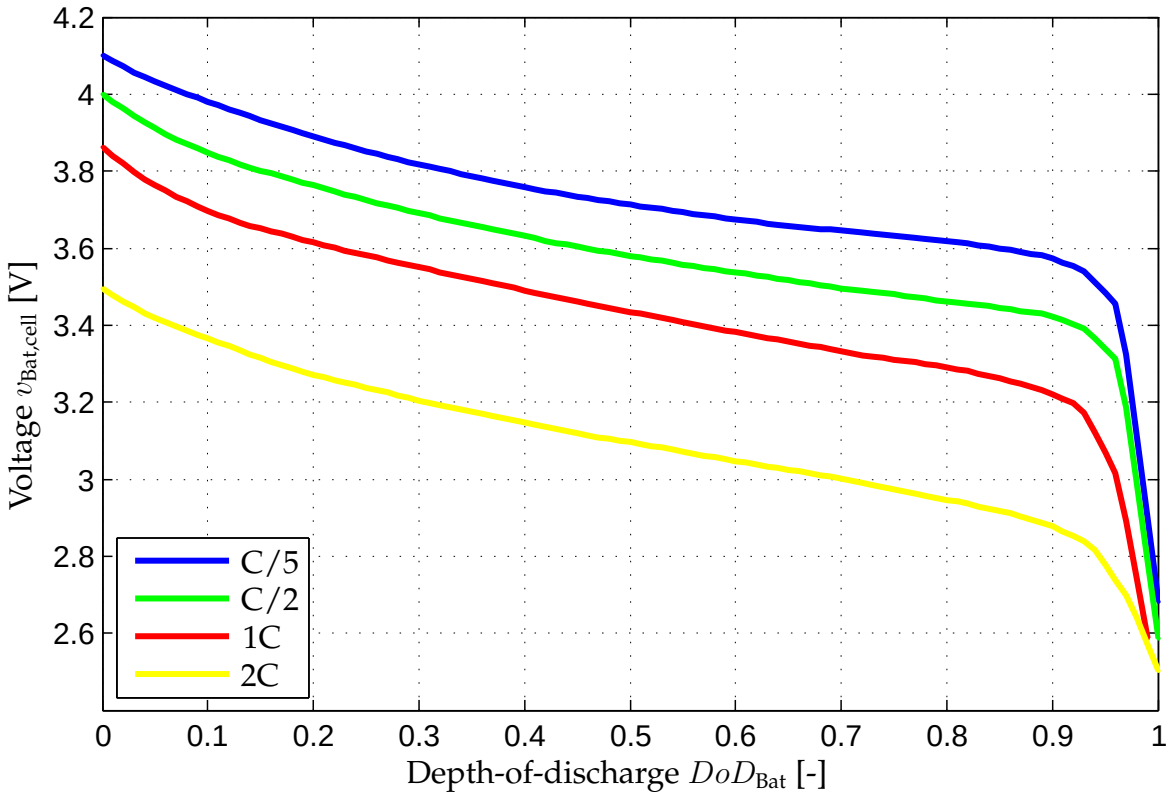

Figure A.4: Voltage versus depth-of-discharge for different discharge current levels.

The battery voltage in Figure A.4 depend on the discharge current and state-of-charge. For two different fractions x_1 and x_2 of the nominal discharge current $I_{\text{Bat,1,cell}}$

the voltage is given

$$v_{\text{Bat,cell}}(x_1 I_{\text{Bat,1,cell}}, DoD_{\text{Bat}}) = v_{\text{Bat,oc,cell}}(DoD_{\text{Bat}}) - R_{\text{Bat,cell,dis}}(DoD_{\text{Bat}}) \cdot x_1 I_{\text{Bat,1,cell}}\,\text{A} \quad [\text{V}] \quad \text{(A.13)}$$

$$v_{\text{Bat,cell}}(x_2 I_{\text{Bat,1,cell}}, DoD_{\text{Bat}}) = v_{\text{Bat,oc,cell}}(DoD_{\text{Bat}}) - R_{\text{Bat,cell,dis}}(DoD_{\text{Bat}}) \cdot x_2 I_{\text{Bat,1,cell}}\,\text{A} \quad [\text{V}] \quad \text{(A.14)}$$

If it is assumed that the inner discharge resistance $R_{\text{Bat,cell,dis}}$ is independent of the current level, the resistance can be calculated from two data sets, i.e.

$$R_{\text{Bat,cell,dis}}(DoD_{\text{Bat}}) = \frac{v_{\text{Bat,cell}}(x_1 I_{\text{Bat,1,cell}}, DoD_{\text{Bat}})}{(x_2 - x_1)\, I_{\text{Bat,1,cell}}} - \frac{v_{\text{Bat,cell}}(x_2 I_{\text{Bat,1,cell}}, DoD_{\text{Bat}})}{(x_2 - x_1)\, I_{\text{Bat,1,cell}}} \quad [\Omega] \quad \text{(A.15)}$$

For each pair of data sets in Figure A.4 the inner discharging resistance $R_{\text{Bat,cell,dis}}$ is calculated. The results can be seen in Figure A.5. It is seen that there are some deviation between the results. This could be because the resistance also is current depending. However, there seems not to be any clear relationship between the resistance and current values. For this reason it is decided to calculate the average resistance for each depth-of-discharge value. The average value is also shown in the figure. It is seen that it increases for higher depth-of-discharge values. The average resistance value can be approximated by a second order polynomial, i.e.

$$R_{\text{Bat,cell,dis}} = a_{10} DoD_{\text{Bat}}^{10} + a_9 DoD_{\text{Bat}}^{9} + a_8 DoD_{\text{Bat}}^{8} + a_7 DoD_{\text{Bat}}^{7} + a_6 DoD_{\text{Bat}}^{6} + a_5 DoD_{\text{Bat}}^{5} + a_4 DoD_{\text{Bat}}^{4} + a_3 DoD_{\text{Bat}}^{3} + a_2 DoD_{\text{Bat}}^{2} + a_1 DoD_{\text{Bat}} + a_0 \quad [\Omega] \quad \text{(A.16)}$$

where

a_{10}	=	-634.0	Constant
a_9	=	2942.1	Constant
a_8	=	-5790.6	Constant
a_7	=	6297.4	Constant
a_6	=	-4132.1	Constant
a_5	=	1677.7	Constant
a_4	=	-416.4	Constant
a_3	=	60.5	Constant
a_2	=	-4.8	Constant
a_1	=	0.2	Constant
a_0	=	0.0	Constant

Open Circuit Voltage

For each data set the internal voltage source $v_{\text{Bat,oc,cell}}$, i.e. the open circuit voltage can be calculated:

$$v_{\text{Bat,oc,cell}} = v_{\text{Bat,cell}} + R_{\text{Bat,cell,dis}} i_{\text{Bat,cell}} \quad [\text{V}] \quad \text{(A.17)}$$

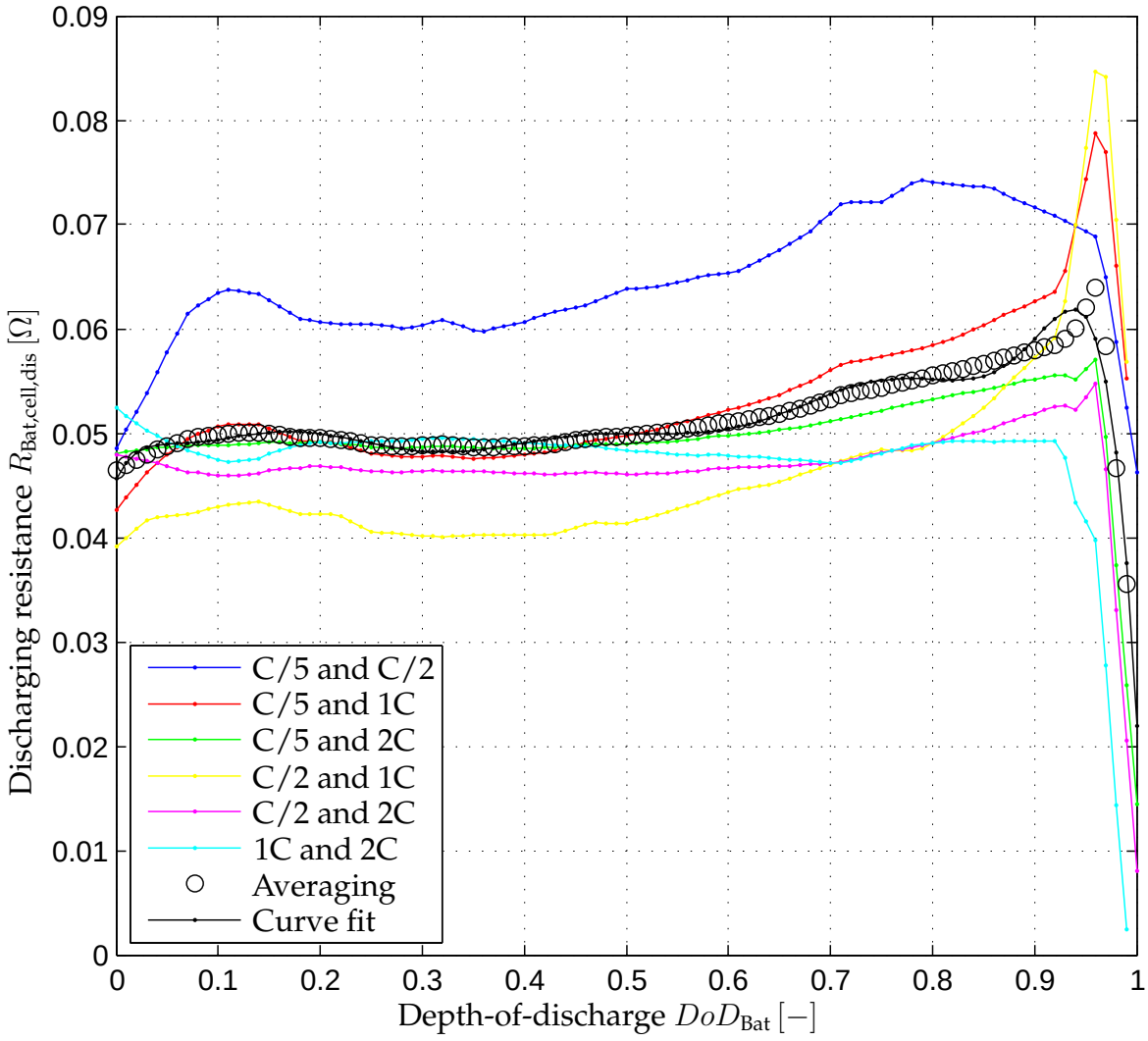

Figure A.5: Inner resistance versus depth-of-discharge calculated from the data sets in Figure A.4.

The results can be seen Fig A.6. The average open circuit voltage can be described by a ten order polynomial. Therefore

$$\begin{aligned} v_{\text{Bat,oc,cell}} =& b_{10} DoD_{\text{Bat}}^{10} + b_9 DoD_{\text{Bat}}^{9} + b_8 DoD_{\text{Bat}}^{8} + b_7 DoD_{\text{Bat}}^{7} \\ &+ b_6 DoD_{\text{Bat}}^{6} + b_5 DoD_{\text{Bat}}^{5} + b_4 DoD_{\text{Bat}}^{4} + b_3 DoD_{\text{Bat}}^{3} \\ &+ b_2 DoD_{\text{Bat}}^{2} + b_1 DoD_{\text{Bat}} + b_0 \qquad [\text{V}] \end{aligned} \tag{A.18}$$

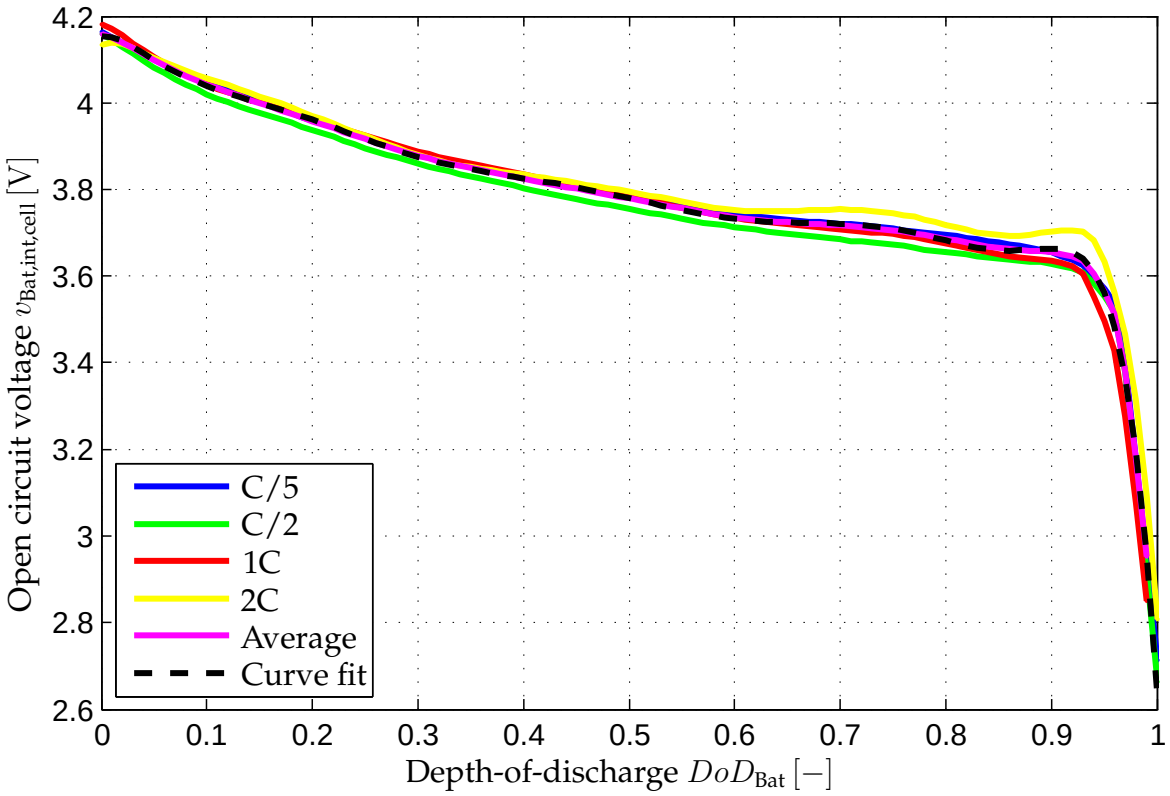

Figure A.6: Calculated open circuit voltage.

where	b_{10}	=	-8848	Constant
	b_9	=	40727	Constant
	b_8	=	-79586	Constant
	b_7	=	86018	Constant
	b_6	=	-56135	Constant
	b_5	=	-5565	Constant
	b_4	=	784	Constant
	b_3	=	-25	Constant
	b_2	=	55	Constant
	b_1	=	0	Constant
	b_0	=	4	Constant

In order to verify the modeling of the inner discharging resistance $R_{\text{Bat,cell,dis}}$ and internal voltage source $v_{\text{Bat,oc,cell}}$ the terminal voltage $v_{\text{Bat,cell}}$ for each of the data set are calculated. Therefore

$$v_{\text{Bat,cell}} = v_{\text{Bat,oc,cell}}(DoD_{\text{Bat}}) - R_{\text{Bat,cell,dis}}(DoD_{\text{Bat}})i_{\text{Bat,cell}} \qquad [\text{V}] \qquad \text{(A.19)}$$

The results can be seen in Figure A.7 where the calculated values and data sheet values are shown as a function of both the capacity and depth-of-discharge. It is seen

that calculations fit the data sheet values. However, for a battery current of $I_{\text{Bat,cell}} = 14.0\,\text{A}$ a deviation is seen for depth-of-discharge values higher than $DoD_{\text{Bat}} = 0.95$.

Charge Efficiency

Due to the Peukert equation the available capacity drops when the drawn current becomes higher than the nominal. During the charging, either from the charging station or due to the regenerative braking, it is important to be able to model how much of the charging current that actually is captured. In Figure A.2 the voltage and state-of-charge are shown for different charging currents. From these data sheet curves, the relationship between that amount of charge that is put into the battery, and that amount of charge that actually is stored, can be calculated. Some of the charging current is "lost". The change in state-of-charge in Figure A.2(c) is the integral of an equivalent charging current $i_{\text{Bat,cell,eq,cha}}$. Therefore

$$\Delta SoC_{\text{Bat}} = -\frac{1}{Q_{\text{Bat,1,cell}}} \int i_{\text{Bat,cell,eq,cha}} dt \qquad [\text{Ah}] \qquad \text{(A.20)}$$

The minus sign is due to the sign convention, where a charging current is negative. The charging current is converted into the equivalent charging current by a charging efficiency $\eta_{\text{Bat,cha}}$, i.e.

$$i_{\text{Bat,cell,eq,cha}} = \eta_{\text{Bat,cha}} i_{\text{Bat,cell}} \qquad [\text{A}] \qquad \text{(A.21)}$$

The charging efficiency is therefore given by

$$\eta_{\text{Bat,cha}} = -\frac{\int i_{\text{Bat,cell}} dt}{\Delta SoC_{\text{Bat}} Q_{\text{Bat,1,cell}}} \qquad [-] \qquad \text{(A.22)}$$

For each data sheet value the efficiency is calculated. The results can be seen in Figure A.8. It is seen that the calculations are with high deviations, which is due to the uncertainty when reading the data sheet curves. However, the charge efficiency does not seem to depend on the charging current or state-of-charge. Therefore the average value is used. The average value is $\eta_{\text{Bat,cha}} = 0.95$, and is also shown in the figure.

Charging Resistance

The charging resistance $R_{\text{Bat,cell,cha}}$ can be calculated from the curves in Figure A.2. Therefore

$$R_{\text{Bat,cell,cha}} = \frac{v_{\text{Bat,oc,cell}} - v_{\text{Bat,cell}}}{i_{\text{Bat,cell}}} \qquad [\Omega] \qquad \text{(A.23)}$$

The open circuit voltage $v_{\text{Bat,oc,cell}}$ is calculated by using the polynomial function in Equation A.18. The result of the charging resistance can be seen in Figure A.9.

The average charing resistance $R_{\text{Bat,cell,cha}}$ is also given by a ten order polynomial, i.e.

$$\begin{aligned} R_{\text{Bat,cell,cha}} = {} & c_{10} DoD_{\text{Bat}}^{10} + c_9 DoD_{\text{Bat}}^{9} + c_8 DoD_{\text{Bat}}^{8} + c_7 DoD_{\text{Bat}}^{7} \\ & + c_6 DoD_{\text{Bat}}^{6} + c_5 DoD_{\text{Bat}}^{5} + c_4 DoD_{\text{Bat}}^{4} + c_3 DoD_{\text{Bat}}^{3} \\ & + c_2 DoD_{\text{Bat}}^{2} + c_1 DoD_{\text{Bat}} + c_0 \qquad [\text{V}] \qquad \text{(A.24)} \end{aligned}$$

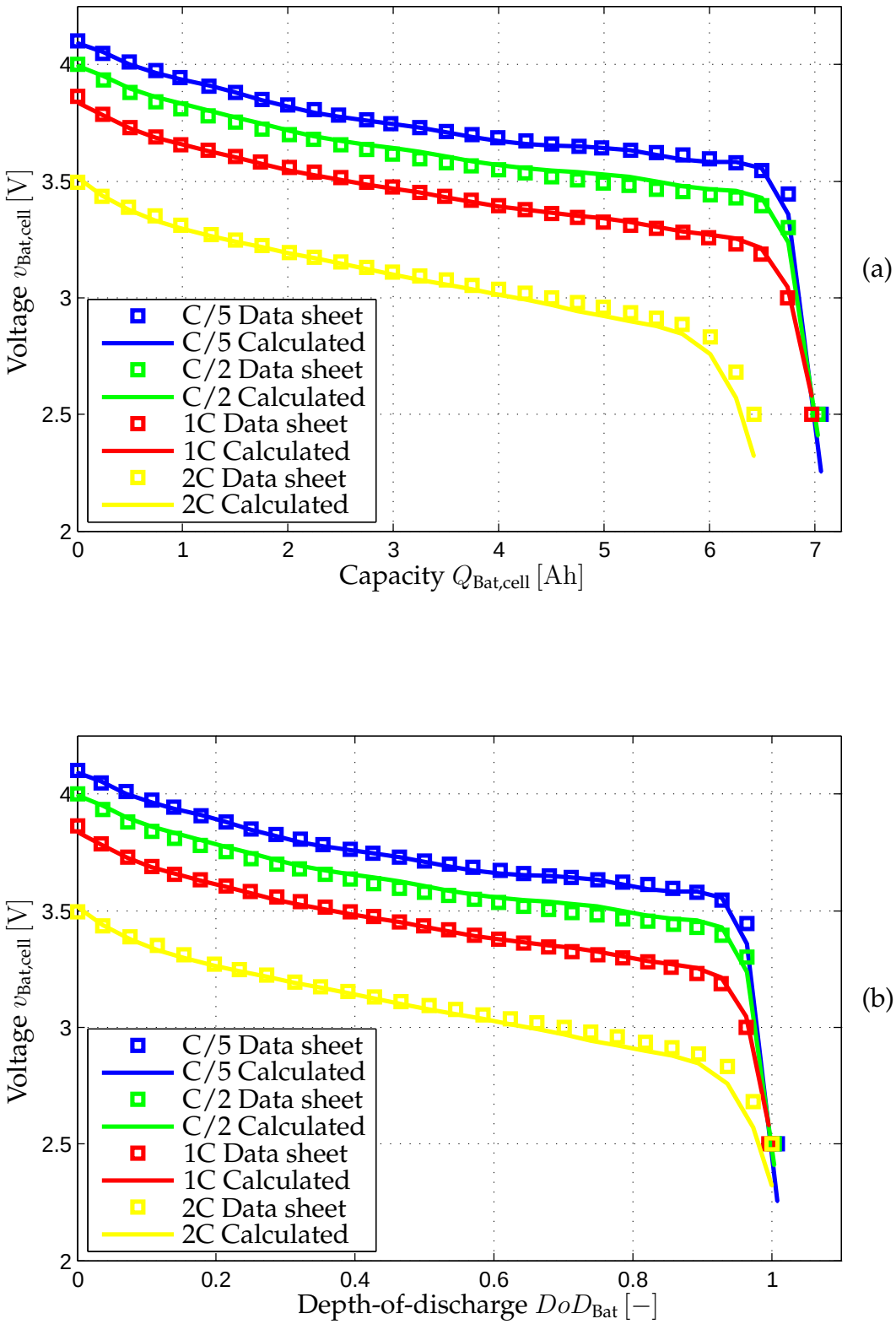

Figure A.7: Data sheet values and calculations of the battery voltage constant discharging currents. (a) Versus the capacity. (b) Versus the depth-of-discharge.

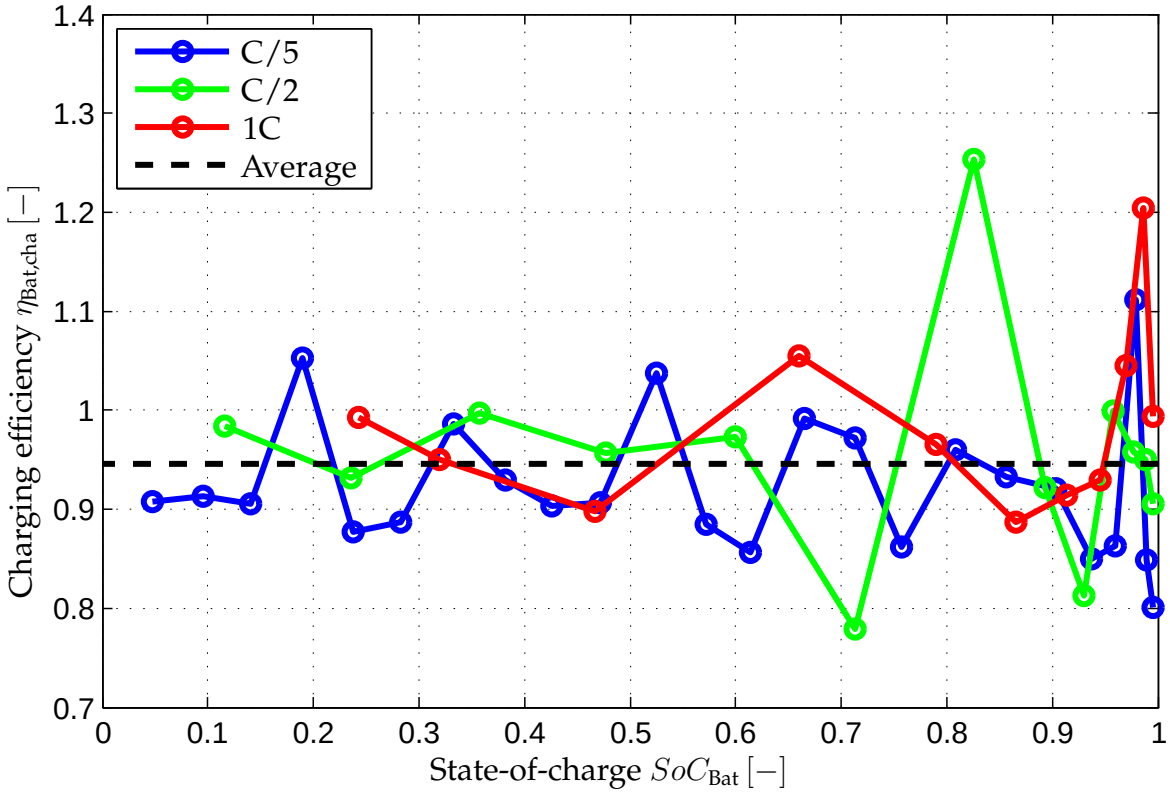

Figure A.8: Calculation of charge efficiency from the data sheet curves in Figure A.2.

where	c_{10}	=	2056	Constant
	c_9	=	-9176	Constant
	c_8	=	17147	Constant
	c_7	=	-17330	Constant
	c_6	=	10168	Constant
	c_5	=	-3415	Constant
	c_4	=	578	Constant
	c_3	=	25	Constant
	c_2	=	3	Constant
	c_1	=	0	Constant
	c_0	=	0	Constant

In order to verify the methods used to calculate the state-of-charge, internal voltage source, and charging resistance calculations are compared to data sheet values. The results can be seen in Figure A.10.

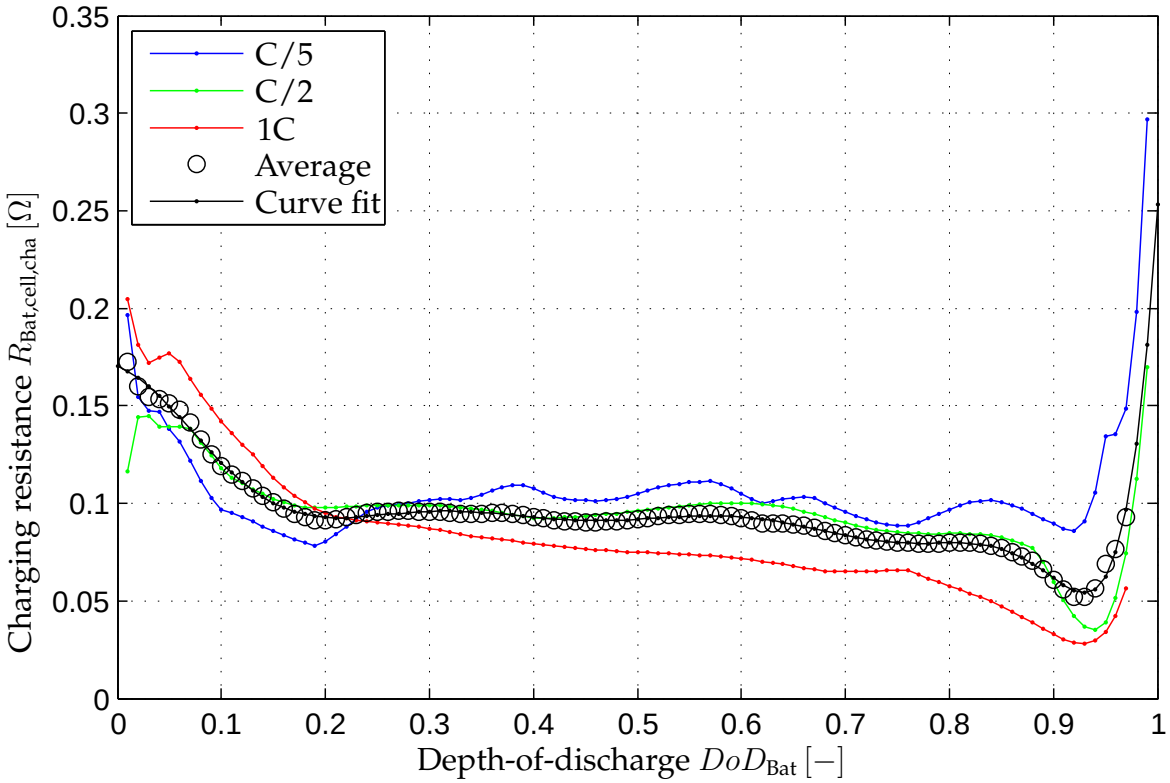

Figure A.9: Calculation of charging resistance from the data sheet curves in Figure A.2.

A.3 CYCLE EFFICIENCY

In order to calculate the cycle efficiency a charging power $p_{\text{Bat,cha}}$ and discharging power $p_{\text{Bat,dis}}$ are defined:

$$p_{\text{Bat,dis}} = \begin{cases} |p_{\text{Bat}}| & p_{\text{Bat}} \geq 0 \\ 0 & p_{\text{Bat}} < 0 \end{cases} \quad [\text{A}] \tag{A.25}$$

$$p_{\text{Bat,cha}} = \begin{cases} |p_{\text{Bat}}| & p_{\text{Bat}} < 0 \\ 0 & p_{\text{Bat}} \geq 0 \end{cases} \quad [\text{A}] \tag{A.26}$$

The cycle efficiency is defined as the energy taken out of the battery relative to the energy entering the battery in order to reach the same state-of-charge level as before the discharging, i.e.

$$\eta_{\text{Bat,cyc}} = \frac{\int_{T_{\text{start}}}^{T_{\text{stop}}} p_{\text{Bat,dis}} dt}{\int_{T_{\text{start}}}^{T_{\text{stop}}} p_{\text{Bat,cha}} dt} 100\,\% \quad [\%] \tag{A.27}$$

$$SoC_{\text{Bat}}\left(T_{\text{start}}\right) = SoC_{\text{Bat}}\left(T_{\text{stop}}\right) \quad [-] \tag{A.28}$$

The cycle efficiency is investigated for different current amplitudes and state-of-charge levels. See Table A.3. The current charging and discharging levels are specified

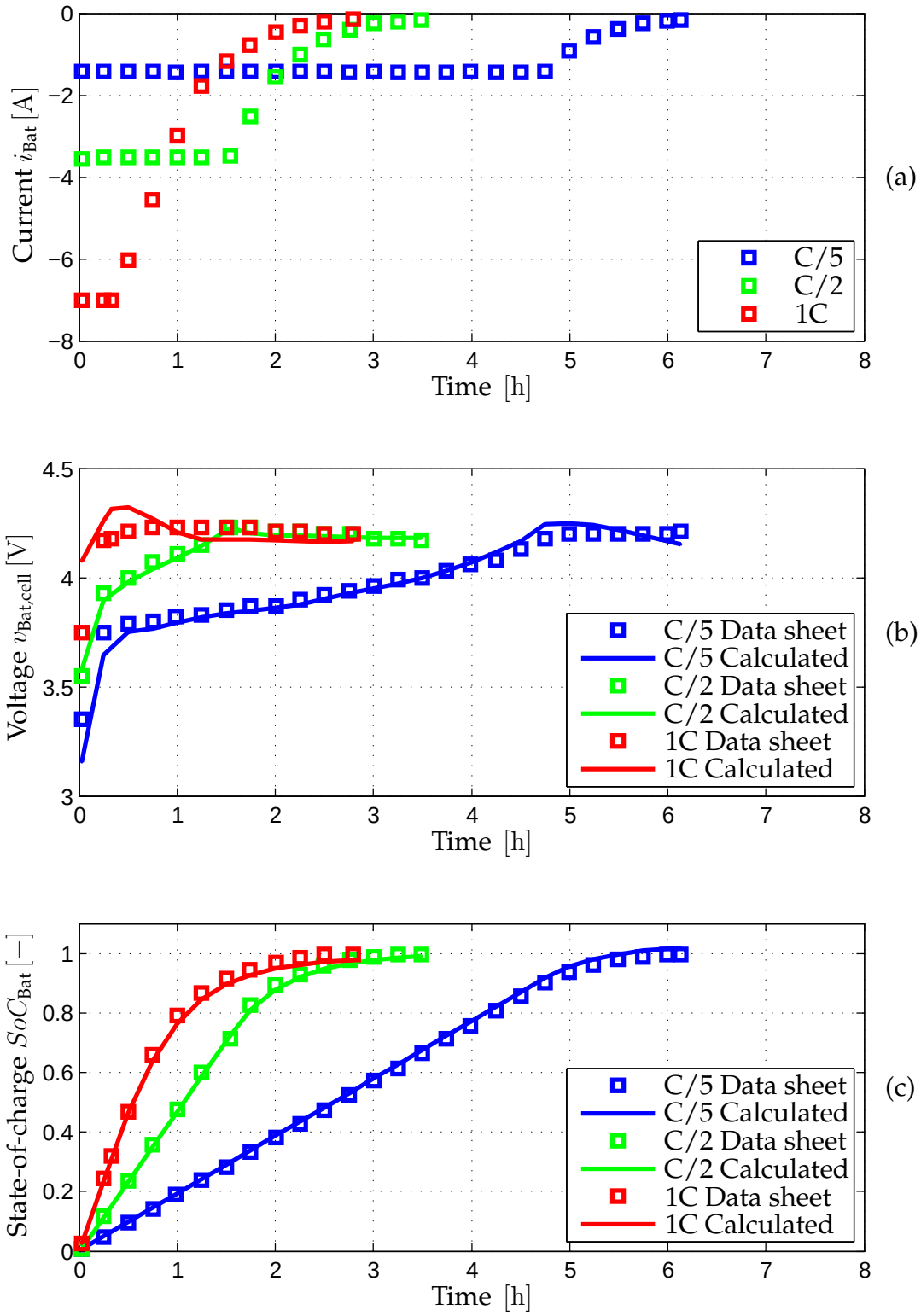

Figure A.10: Simulation and data sheet comparison. (a) Charging current. (b) Battery voltage. (c) State-of-charge.

Charge/discharge current [A]	Minimum state-of-charge [%]				
	0	20	40	60	80
C/5	89.9	90.0	90.0	90.1	90.3
C/2	84.1	84.4	84.8	85.6	87.4
1C	77.7	79.0	80.2	81.6	83.5
2C	63.6	65.2	66.2	67.8	69.5

Table A.3: Cycle efficiency of battery cell in percentage for different charge/discharge ratings and minimum state-of-charge levels.

in terms of C. However, during the charging the specified current in the table will only be used if it is equal to or less than the recommended charging current of 1C, and if the battery voltage is below or equal to the maximum allowed limit.

B Electric Machine

B.1 MODELING

The electric model of the PMSM is given by

$$v_{\mathrm{d}} = R_{\mathrm{s}} i_{\mathrm{d}} + L_{\mathrm{d}} \frac{di_{\mathrm{d}}}{dt} - \omega_e L_{\mathrm{q}} i_{\mathrm{q}} \tag{B.1}$$

$$v_{\mathrm{q}} = R_{\mathrm{s}} i_{\mathrm{q}} + L_{\mathrm{q}} \frac{di_{\mathrm{q}}}{dt} + \omega_e L_{\mathrm{d}} i_{\mathrm{d}} + \omega_{\mathrm{e}} \lambda_{pm} \tag{B.2}$$

$$p_{\mathrm{e}} = \frac{3}{2} \left(v_{\mathrm{d}} i_{\mathrm{d}} + v_{\mathrm{q}} i_{\mathrm{q}} \right) \tag{B.3}$$

where	v_{d}	[V]	D-axis voltage
	v_{q}	[V]	Q-axis voltage
	i_{d}	[A]	D-axis current
	i_{q}	[A]	Q-axis current
	R_{s}	[Ω]	Stator phase resistance
	L_{d}	[H]	D-axis inductance
	L_{q}	[H]	Q-axis inductance
	λ_{pm}	[Wb]	Permanent magnet flux linkage
	ω_{e}	[rad/s]	Angular frequency of the stator
	λ_{pm}	[Wb]	Permanent magnet flux linkage
	p_{e}	[W]	Electric input power

The mechanical part of the PMSM can be modeled as follows:

$$\tau_{\mathrm{e}} = J_{\mathrm{s}} \frac{d\omega_{\mathrm{s}}}{dt} + \tau_{\mathrm{v}} + \tau_{\mathrm{c}} + \tau_{\mathrm{s}} \tag{B.4}$$

$$\tau_{\mathrm{v}} = B_{\mathrm{v}} \omega_{\mathrm{s}} \tag{B.5}$$

$$p_{\mathrm{s}} = \tau_{\mathrm{s}} \omega_{\mathrm{s}} \tag{B.6}$$

where	ω_s	$[\mathrm{rad/s}]$	Shaft angular velocity
	J_s	$[\mathrm{kgm}^2]$	Shaft moment of inertia
	τ_e	$[\mathrm{Nm}]$	Electromechanical torque
	τ_s	$[\mathrm{Nm}]$	Shaft torque
	τ_c	$[\mathrm{Nm}]$	Coulomb torque
	B_v	$[\mathrm{Nms/rad}]$	Viscous friction coefficient
	P	$[-]$	Number of poles
	p_s	$[\mathrm{W}]$	Shaft power

The coupling between the electric and mechanical part is

$$\tau_\mathrm{e} = \frac{3}{2}\frac{P}{2}\left(\lambda_{pm} i_\mathrm{q} + \left(L_\mathrm{d} - L_\mathrm{q}\right) i_\mathrm{d} i_\mathrm{q}\right) \tag{B.7}$$

$$\omega_\mathrm{e} = \frac{P}{2}\omega_\mathrm{s} \tag{B.8}$$

Simplified Model

Many options exist for controlling the PMSM. In order to simplify it is chosen to use the $I_\mathrm{d} = 0$ control. Thereby the reluctance torque cannot be utilized, but the reluctance contribution is usually minor in compare to the torque of the permanent magnet. The mechanical and electric time constants are much smaller of the electric machine than for the vehicle it self. The electric machine are therefore considered to operate in steady-state. With the $I_d = 0$ property the electric machine model is therefore reduced to

$$v_\mathrm{d} = R_\mathrm{s} i_\mathrm{d} - \omega_\mathrm{e} L_\mathrm{q} i_\mathrm{q} \quad [\mathrm{V}] \tag{B.9}$$

$$v_\mathrm{q} = R_\mathrm{s} i_\mathrm{q} + \omega_\mathrm{e} \lambda_\mathrm{pm} \quad [\mathrm{V}] \tag{B.10}$$

$$p_\mathrm{e} = \frac{3}{2} v_\mathrm{q} i_\mathrm{q} \quad [\mathrm{W}] \tag{B.11}$$

$$\tau_\mathrm{e} = B_\mathrm{v}\omega_\mathrm{s} + \tau_\mathrm{c} + \tau_\mathrm{s} \quad [\mathrm{Nm}] \tag{B.12}$$

$$p_\mathrm{s} = \tau_\mathrm{s}\omega_\mathrm{s} \quad [\mathrm{W}] \tag{B.13}$$

Several modulation techniques also exist for inverting the DC bus voltage to three phase AC voltage. The different techniques has different performances in the usage of the bus voltage, harmonic content, acoustic noise, etc. Again, due to the simple implementation, the sinusoidal pulse width modulation (PWM) technique is chosen.

When using sinusoidal modulation the phase peak is

$$\hat{V}_\mathrm{p} = m_\mathrm{i}\frac{V_\mathrm{Bus}}{2} \tag{B.14}$$

where	$\hat{V}_\mathrm{p}$	$[\mathrm{V}]$	Phase peak voltage
	m_i	$[-]$	Modulation index
	V_Bus	$[\mathrm{V}]$	Bus voltage

B.2 DESIGN

In order to design the machine design constraints from UQM Technologies [18] are applied. The machine from UQM Technologies is a brushless permanent magnet synchronous machine with the specifications in Table B.1.

Continuous shaft power ($4000\,\mathrm{rpm}$)	$P_{\mathrm{s,cont}}$	$45\,\mathrm{kW}$
Peak shaft power	$P_{\mathrm{s,max}}$	$75\,\mathrm{kW}$
Maximum speed	$n_{\mathrm{s,max}}$	$8000\,\mathrm{rpm}$
Number of poles [8]	P	18
Continuous shaft torque	$\tau_{\mathrm{s,cont}}$	$150\,\mathrm{Nm}$
Peak shaft torque	$\tau_{\mathrm{s,max}}$	$240\,\mathrm{Nm}$
Nominal efficiency	$\eta_{\mathrm{EM,nom}}$	$94\,\%$
Specific power (based on peak power)	$\mathrm{SP_{EM}}$	$1.83\,\mathrm{kW/kg}$
Power density (based on peak power)	$\mathrm{PD_{EM}}$	$4.83\,\mathrm{kW/L}$
Maximum shaft torque at maximum speed (based on approximation from data sheet)	$\tau_{\mathrm{s,max},\omega_{\mathrm{s,max}}}$	$85\,\mathrm{Nm}$
Maximum shaft speed at continuous torque (based on approximation from data sheet)	$n_{\mathrm{s,max},\tau_{\mathrm{s,cont}}}$	$4775\,\mathrm{rpm}$

Table B.1: Specifications of UQM PowerPhase 75 [18].

The phase angle between the voltage and current is not specified, but is assumed to be $\phi_{\mathrm{EM,nom}} = 0.55\,\mathrm{rad}$, which corresponds to a power factor of $\cos(\phi_{\mathrm{EM}}) = 0.85$.

Based on the specifications of the UQM the following relationships can be defined

$$a_{\mathrm{EM},1} = \frac{\tau_{\mathrm{s,max}}}{\tau_{\mathrm{s,cont}}} = \frac{240\,\mathrm{Nm}}{150\,\mathrm{Nm}} = 1.6 \tag{B.15}$$

$$a_{\mathrm{EM},2} = \frac{\tau_{\mathrm{s,max}}}{\tau_{\mathrm{s,max},\omega_{\mathrm{s,max}}}} = \frac{240\,\mathrm{Nm}}{85\,\mathrm{Nm}} = 2.82 \tag{B.16}$$

$$a_{\mathrm{EM},3} = \frac{n_{\mathrm{s,max}}}{n_{\mathrm{s,max},\tau_{\mathrm{s,cont}}}} = \frac{8000\,\mathrm{rpm}}{4775\,\mathrm{rpm}} = 1.6754 \tag{B.17}$$

The relation ships in Equation (B.15)-(B.17) will be used as design constraints. At full power and maximum speed is the efficiency $\eta_{\mathrm{EM}} \approx 0.9$ of the UQM machine [18]. The maximum efficiency of the should be located around the nominal point of operation. By try-and-error-method it turns out that if the coulomb torque and viscous friction are responsible for $2\,\%$ and $6\,\%$, respectively, of the power loss at full power and maximum speed, the maximum efficiency is located around the nominal point of operation. Therefore

$$\tau_{\mathrm{c}} = \frac{0.02}{\omega_{\mathrm{s}}} \frac{P_{\mathrm{s,max}}}{0.9} \qquad [\mathrm{Nm}] \tag{B.18}$$

$$B_{\mathrm{v}} = \frac{0.06}{\omega_{\mathrm{s}}^2} \frac{P_{\mathrm{s,max}}}{0.9} \qquad [\mathrm{Nms/rad}] \tag{B.19}$$

As the maximum speed have been selected to $n_{\text{s,max}} = 8000\,\text{rpm}$ are the maximum speed at continuous torque and angular velocities given by

$$n_{\text{s,max},\tau_{\text{s,cont}}} = \frac{n_{\text{s,max}}}{a_{\text{EM,3}}} = \frac{8000\,\text{rpm}}{1.6754} = 4775\,\text{rpm} \tag{B.20}$$

$$\omega_{\text{s,max},\tau_{\text{s,cont}}} = n_{\text{s,max},\tau_{\text{s,cont}}} \frac{2\pi}{60\,\text{s/min}} = 4775\,\text{rpm} \frac{2\pi}{60\,\text{s/min}} = 500\,\text{rad/s} \tag{B.21}$$

$$\omega_{\text{e,max},\tau_{\text{s,cont}}} = \frac{P}{2}\omega_{\text{s,max},\tau_{\text{s,cont}}} = \frac{18}{2} 500\,\text{rad/s} = 4500\,\text{rad/s} \tag{B.22}$$

There are two torque requirements, i.e. maximum torque at maximum speed $\tau_{\text{s,max},\omega_{s,max}}$ for driving at maximum speed, and maximum torque $\tau_{\text{s,max}}$ for the accelerations and decelerations. The motor is therefore designed after that force that provides the highest requirement, i.e. if $f_{\text{t,req,max}}$ is the highest required traction force for the given driving cycle, and $f_{\text{t,req,nom}}$ is the required traction force at maximum speed, the maximum traction force $f_{\text{t,max}}$ and traction torque $\tau_{\text{t,max}}$ are

$$f_{\text{t,max}} = 1.05 \cdot max\left(\begin{bmatrix} f_{\text{t,req,max}} \\ a_{\text{EM,2}} f_{t,req,nom} \end{bmatrix}\right) \qquad [\text{N}] \tag{B.23}$$

$$\tau_{\text{t,max}} = f_{\text{t,max}} r_w \qquad [\text{Nm}] \tag{B.24}$$

It is noticed that the nominal and maximum traction force have a buffer of $5\,\%$ to the needed.

The maximum and nominal shaft torques are therefore

$$\tau_{\text{s,max}} = \frac{\tau_{\text{t,max}}}{\eta_{\text{tra}}} \qquad [\text{Nm}] \tag{B.25}$$

$$\tau_{\text{s,cont}} = \frac{\tau_{\text{s,max}}}{a_{\text{EM,1}}} \qquad [\text{Nm}] \tag{B.26}$$

The nominal electro mechanical torque is:

$$\tau_{\text{e,cont}} = \tau_{\text{c}} + B_{\text{v}} \omega_{\text{s,max},\tau_{\text{s,cont}}} + \tau_{s,cont} \qquad [\text{Nm}] \tag{B.27}$$

The machine will be designed at continuous torque speed $\omega_{\text{s,cont}}$, maximum power $P_{\text{s,max}}$, nominal efficiency $\eta_{\text{EM,nom}}$, and minimum bus voltage $V_{\text{Bus,min}}$. The speed is approximately proportional to the terminal voltage. At the minimum bus voltage the machine should be able run at maximum speed with a modulation index $m_{\text{i}} = 1$. Because the machine is designed at nominal speed, but at the minimum bus voltage, the modulation index is $m_{\text{i,nom}} = \frac{1}{a_{\text{EM,3}}} = 0.3581$. The voltages of the machine is therefore:

$$\hat{V}_{\text{p,nom}} = m_{\text{i,nom}} \frac{V_{\text{Bus,min}}}{2} \qquad [\text{V}] \tag{B.28}$$

$$V_{\text{d,nom}} = -\hat{V}_{\text{p,nom}} \sin(\phi_{\text{EM,nom}}) \qquad [\text{V}] \tag{B.29}$$

$$V_{\text{q,nom}} = \hat{V}_{\text{p,nom}} \cos(\phi_{\text{EM,nom}}) \qquad [\text{V}] \tag{B.30}$$

Therefore, at $I_{\mathrm{d}} = 0$ control the machine parameters can be designed as follows:

$$P_{\mathrm{s,max}} = \omega_{\mathrm{s,max},\tau_{\mathrm{s,cont}}} \tau_{\mathrm{s,cont}} \quad [\mathrm{W}] \tag{B.31}$$

$$P_{\mathrm{e,max}} = \frac{P_{\mathrm{s,max}}}{\eta_{\mathrm{EM,nom}}} \quad [-] \tag{B.32}$$

$$I_{\mathrm{q,cont}} = \frac{2}{3} \frac{P_{\mathrm{e,cont}}}{V_{\mathrm{q,nom}}} \quad [\mathrm{A}] \tag{B.33}$$

$$\lambda_{\mathrm{pm}} = \frac{2}{3} \frac{2}{P} \frac{\tau_{\mathrm{e,cont}}}{I_{\mathrm{q,cont}}} \quad [\mathrm{Wb}] \tag{B.34}$$

$$L_{\mathrm{q}} = -\frac{V_{\mathrm{d,nom}}}{\omega_{\mathrm{e,max},\tau_{\mathrm{s,cont}}} I_{\mathrm{q,nom}}} \quad [\mathrm{H}] \tag{B.35}$$

$$R_{\mathrm{s}} = \frac{V_{\mathrm{q,nom}} - \omega_{\mathrm{e,max},\tau_{\mathrm{s,cont}}} \lambda_{\mathrm{pm}}}{I_{\mathrm{q,cont}}} \quad [\Omega] \tag{B.36}$$

The efficiency of the machine for different torque-speed characteristics can be seen in Figure B.1.

The efficiency of the machine for different power-speed characteristics can be seen in Figure B.2.

The rated electric machine power is

$$P_{\mathrm{EM,rat}} = P_{\mathrm{s,max}} \quad [\mathrm{W}] \tag{B.37}$$

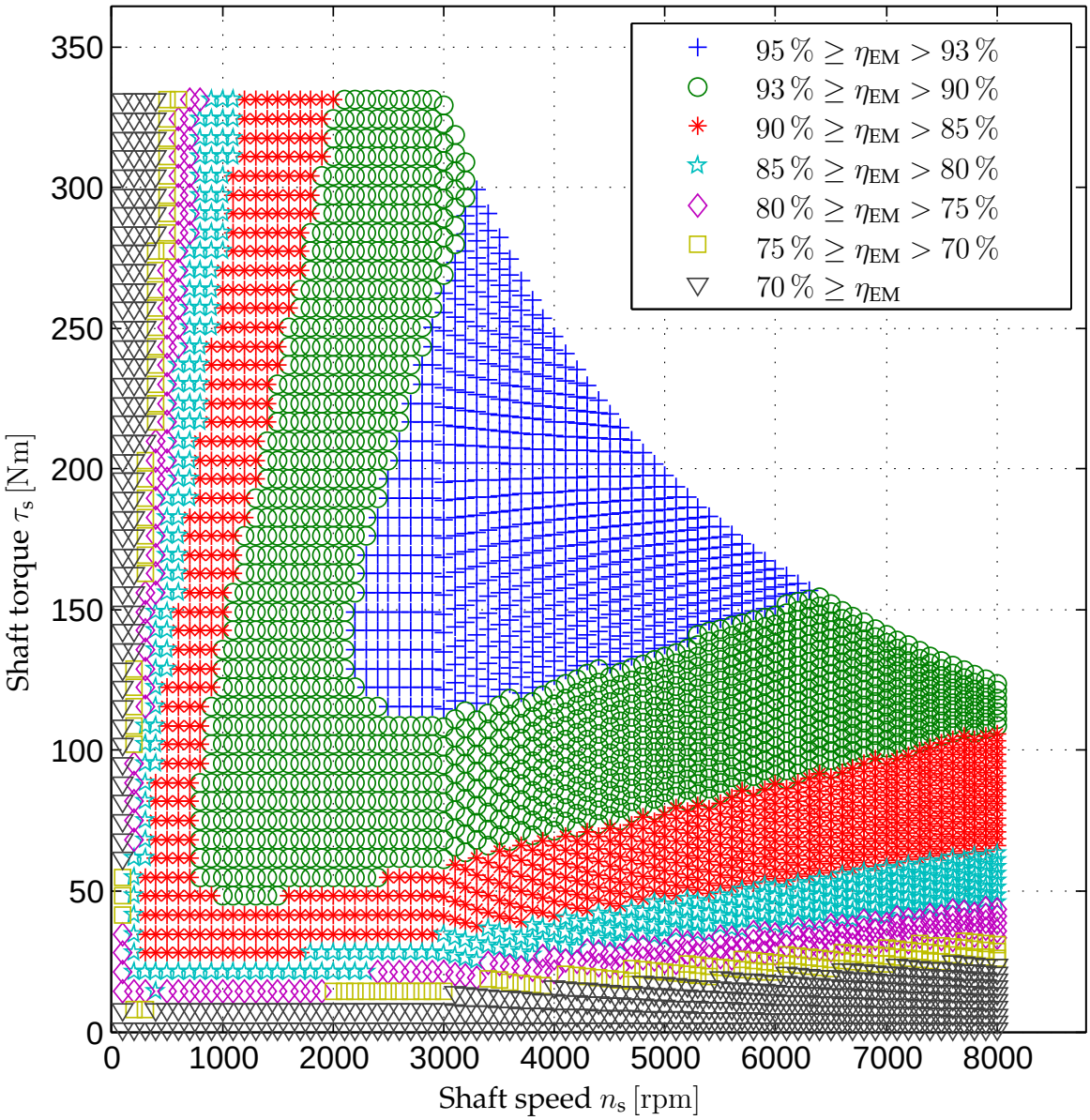

Figure B.1: Efficiency of the electric machine.

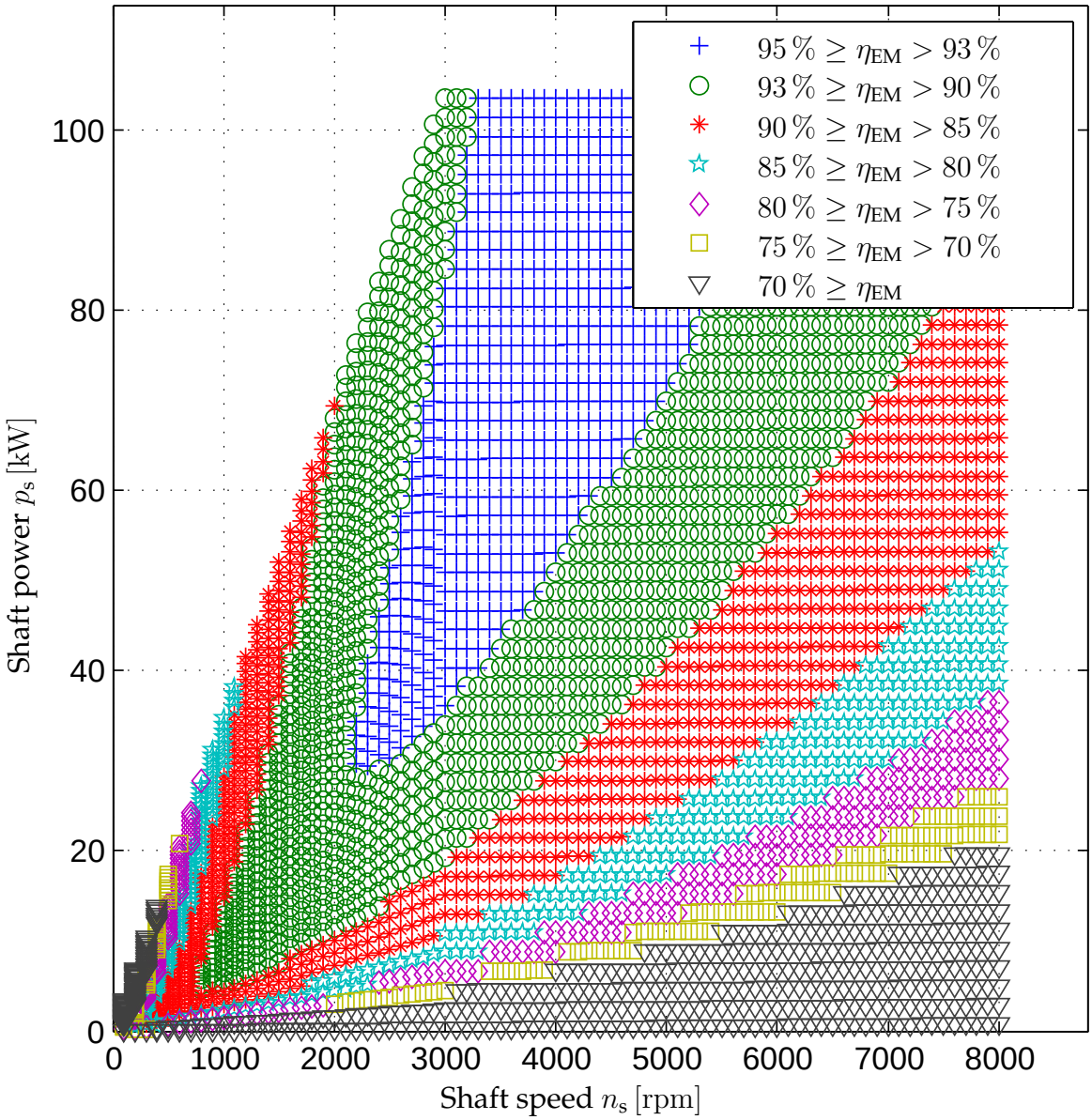

Figure B.2: Efficiency of the electric machine.

C Transmission

The used driving cycle only considers the case where the vehicle is going straight ahead, i.e. the speed and torque of each driving wheel are therefore the same. Therefore

$$\tau_{\mathrm{t}} = f_{\mathrm{t}} r_{\mathrm{w}} \tag{C.1}$$

$$\tau_{\mathrm{w}} = \frac{\tau_{\mathrm{t}}}{2} \tag{C.2}$$

$$\omega_{\mathrm{w}} = \frac{v_{\mathrm{car}}}{r_{\mathrm{w}}} \tag{C.3}$$

$$p_{\mathrm{t}} = f_{\mathrm{t}} v_{\mathrm{car}} \tag{C.4}$$

where	τ_{t}	$[\mathrm{Nm}]$	Traction torque
	τ_{w}	$[\mathrm{Nm}]$	Torque of each driving wheel
	ω_{w}	$[\mathrm{rad/s}]$	Angular velocity of the wheels
	p_{t}	$[\mathrm{W}]$	Traction power

Due to the lack of better data, it is assumed that the power from the shaft of the electric motor to the two driving wheels has a constant efficiency of $\eta_{\mathrm{TS}} = 0.95$ [5]. Therefore

$$\tau_{\mathrm{s}} = \begin{cases} \eta_{\mathrm{TS}} \frac{\tau_{\mathrm{t}}}{G} & p_{\mathrm{t}} < 0 \\ \frac{\tau_{\mathrm{t}}}{\eta_{\mathrm{TS}} G} & p_{\mathrm{t}} \geq 0 \end{cases} \qquad [\mathrm{Nm}] \tag{C.5}$$

The angular shaft velocity of the electric machine ω_s is

$$\omega_{\mathrm{s}} = G \omega_w \qquad [\mathrm{rad/s}] \tag{C.6}$$

The maximum vehicle speed is $V_{car,max} = \frac{200\,\mathrm{km/h}}{3.6\,\mathrm{ks/h}} = 55.6\,\mathrm{m/s}$, and the maximum speed of the electric machine has been set to $n_{\mathrm{s,max}} = 8000\,\mathrm{rpm}$. The required gear ratio of the differential is therefore

$$G = \frac{n_{\mathrm{s,max}}}{V_{\mathrm{car,max}} \frac{1}{r_{\mathrm{w}}} \frac{60}{2\pi}} \approx 5 \tag{C.7}$$

D Inverter

A circuit diagram of the inverter can be seen in Figure D.1. The inverter transmit power between the electric machine (with phase voltages v_{A}, v_{B}, and v_{C}) and the bus by turning on and off the switches $Q_{\mathrm{A+}}$, $Q_{\mathrm{A-}}$, $Q_{\mathrm{B+}}$, $Q_{\mathrm{B-}}$, $Q_{\mathrm{C+}}$, and $Q_{\mathrm{C-}}$. The switches has an on-resistance $R_{\mathrm{Q,Inv}}$. The diodes in parallel of each switch are creating a path for the motor currents during the deadtime, i.e. the time where both switches in one branch are non-conducting in order to avoid a shoot-through.

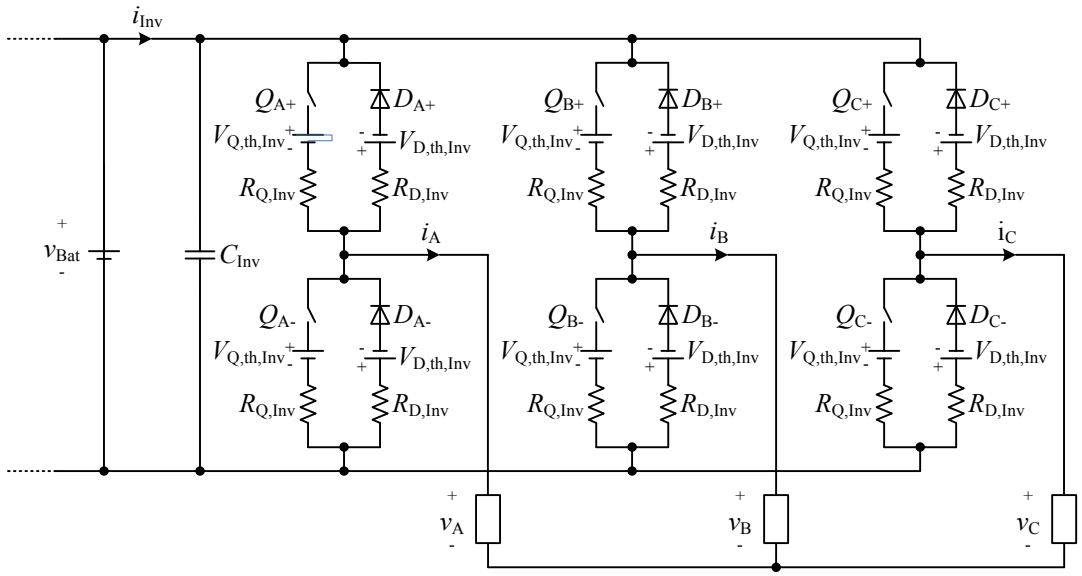

Figure D.1: Circuit diagram of inverter.

Voltage Modeling

The inverter inverts the DC bus voltage to three phase AC voltages and currents, which are given by

$$v_{\mathrm{A}} = \hat{V}_{\mathrm{p}} \sin\left(\omega_{\mathrm{e}} t + \phi_{\mathrm{EM}}\right) \quad [\mathrm{V}] \tag{D.1}$$

$$v_{\mathrm{B}} = \hat{V}_{\mathrm{p}} \sin\left(\omega_{\mathrm{e}} t + \frac{2\pi}{3} + \phi_{\mathrm{EM}}\right) \quad [\mathrm{V}] \tag{D.2}$$

$$v_{\mathrm{C}} = \hat{V}_{\mathrm{p}} \sin\left(\omega_{\mathrm{e}} t - \frac{2\pi}{3} + \phi_{\mathrm{EM}}\right) \quad [\mathrm{V}] \tag{D.3}$$

$$i_{\mathrm{A}} = \hat{I}_{\mathrm{p}} \sin\left(\omega_{\mathrm{e}} t\right) \quad [\mathrm{A}] \tag{D.4}$$

$$i_{\mathrm{B}} = \hat{I}_{\mathrm{p}} \sin\left(\omega_{\mathrm{e}} t + \frac{2\pi}{3}\right) \quad [\mathrm{A}] \tag{D.5}$$

$$i_{\mathrm{C}} = \hat{I}_{\mathrm{p}} \sin\left(\omega_{\mathrm{e}} t - \frac{2\pi}{3}\right) \quad [\mathrm{A}] \tag{D.6}$$

where	$\hat{V}_{\mathrm{p}}$	[V]	Peak phase voltage
	$\hat{I}_{\mathrm{p}}$	[A]	Peak phase current
	ϕ_{EM}	[rad]	Power factor angle
	ω_{e}	[rad/s]	Fundamental angular velocity

Many modulation methods that can do the DC/AC conversion exist. A simple method is the sinusoidal modulation. When using this method the duty cycle $d_{\mathrm{A+}}$ of the upper switch $Q_{\mathrm{A+}}$ of branch A is given by [11]

$$d_{\mathrm{A+}} = \frac{1}{2}\left(1 + \frac{v_{\mathrm{A}}}{\frac{V_{\mathrm{Bus}}}{2}}\right) = \frac{1}{2}\left(1 + \underbrace{\frac{\hat{V}_{\mathrm{p}}}{\frac{V_{\mathrm{Bus}}}{2}}}_{m_{\mathrm{i}}} \sin\left(\omega_{\mathrm{e}} t + \phi_{\mathrm{EM}}\right)\right) \tag{D.7}$$

$$= \frac{1}{2}\left(1 + m_{\mathrm{i}} \sin\left(\omega_{\mathrm{e}} t + \phi_{\mathrm{EM}}\right)\right) \quad [-] \tag{D.8}$$

where	v_{A}	[V]	Voltage of phase A
	m_{i}	[−]	Modulation index

The duty cycle of the two other phases are shifted $120\,^{\circ}$ with reference to phase A.

Loss Modeling

The average power losses of one switch $p_{\mathrm{Q,Inv}}$ and diode $p_{\mathrm{D,Inv}}$ in Figure D.1 during one fundamental period are [3]: The power of the switch $Q_{\mathrm{U,A}}$ and diode $D_{\mathrm{L,A}}$ is therefore given by loss due to the forward voltages and internal resistances, i.e.

$$p_{\mathrm{Q,Inv}} = \left(\frac{1}{8} + \frac{m_{\mathrm{i}}}{3\pi}\right) R_{\mathrm{Q,Inv}} \hat{I}_{\mathrm{p}}^2 + \left(\frac{1}{2\pi} + \frac{m_{\mathrm{i}}}{8}\cos(\phi_{\mathrm{EM}})\right) V_{\mathrm{Q,th,Inv}} \hat{I}_p \quad [\mathrm{W}] \tag{D.9}$$

$$p_{\mathrm{D,Inv}} = \left(\frac{1}{8} - \frac{m_{\mathrm{i}}}{3\pi}\right) R_{\mathrm{D,Inv}} \hat{I}_{\mathrm{p}}^2 + \left(\frac{1}{2\pi} - \frac{m_{\mathrm{i}}}{8}\cos(\phi_{\mathrm{EM}})\right) V_{D,th,Inv} \hat{I}_{\mathrm{p}} \quad [\mathrm{W}] \tag{D.10}$$

If it is assumed that the threshold voltage drop of the switches $V_{\mathrm{Q,th,Inv}}$ and diodes $V_{\mathrm{D,th,Inv}}$ are equal, i.e. $V_{\mathrm{th,Inv}} = V_{\mathrm{Q,th,Inv}} = V_{\mathrm{D,th,Inv}}$, and that the resistances of the

switches $R_{\text{Q,Inv}}$ and diodes $R_{\text{D,Inv}}$ also are equal, i.e. $R_{\text{Inv}} = R_{\text{Q,Inv}} = R_{\text{D,Inv}}$, the total power loss of the inverter is given by

$$P_{\text{Inv,loss}} = 6\left(P_{\text{Q,Inv}} + P_{\text{D,Inv}}\right) = \frac{3}{2} R_{\text{Inv}} \hat{I}_{\text{p}}^2 + \frac{6}{\pi} V_{\text{th,Inv}} \hat{I}_{\text{p}} \qquad [\text{W}] \tag{D.11}$$

The output power of the inverter is the motor input power p_{EM}. The inverter input power P_{Inv} and efficiency is therefore

$$p_{\text{Inv}} = v_{\text{Bus}} i_{\text{Inv}} = p_{\text{EM}} + p_{\text{Inv,loss}} \qquad [\text{W}] \tag{D.12}$$

$$\eta_{\text{Inv}} = \begin{cases} \frac{p_{\text{EM}}}{p_{\text{Inv}}} & p_{\text{EM}} \geq 0 \\ \frac{p_{\text{Inv}}}{p_{\text{EM}}} & p_{\text{EM}} < 0 \end{cases} \qquad [-] \tag{D.13}$$

Design

The inverter is designed at the same point of operation as the electric machine, i.e. nominal machine power $P_{\text{e,nom}}$ and minimum bus voltage $V_{\text{Bus,min}}$. The inverter is designed to have an efficiency of $\eta_{\text{Inv,nom}} = 0.95$ at that point of operation. The loss $P_{\text{Inv,loss,nom}}$ and resistance R_{Inv} of the inverter is therefore

$$P_{\text{Inv,loss,nom}} = \frac{1 - \eta_{\text{Inv,nom}}}{\eta_{\text{Inv,nom}}} P_{\text{EM,nom}} \qquad [\text{W}] \tag{D.14}$$

$$R_{\text{Inv}} = \frac{P_{\text{Inv,loss,nom}} - \frac{6}{\pi} V_{\text{th,Inv}} \hat{I}_{\text{p}}}{\frac{3}{2} \hat{I}_{\text{p}}^2} \qquad [\Omega] \tag{D.15}$$

The threshold voltage is assumed to be $V_{\text{th,Inv}} = 1\,\text{V}$.

Mass and Volume

In order to be able to calculate the mass and volume the specifications in Table D.1 are used.

Description	Symbol	Value
Peak specific power (Toyota Camry [12])	SP_{Inv}	$9.3\,\text{kW/kg}$
Peak power density (Toyota Camry [12])	PD_{Inv}	$11.7\,\text{kW/L}$

Table D.1: Specifications of Toyota Camry inverter.

The inverter VA-rating depend on the battery voltage and current. It is chosen to have a buffer of $20\,\%$ of the inverter voltage and current. The inverter peak power rating is therefore

$$P_{\text{Inv,rat}} = 1.2 V_{\text{Bat,max}} 1.2 I_{\text{Bat,max}} \qquad [\text{W}] \tag{D.16}$$

E Rectifier

In order to utilize the three phase voltages of the grid v_{U}, v_{V}, and v_{W} they are rectified by a rectifier as seen in Figure E.1. In the rectifier the loss is due to the resistance $R_{\mathrm{D,RF}}$ and threshold voltage $V_{\mathrm{D,th,RF}}$.

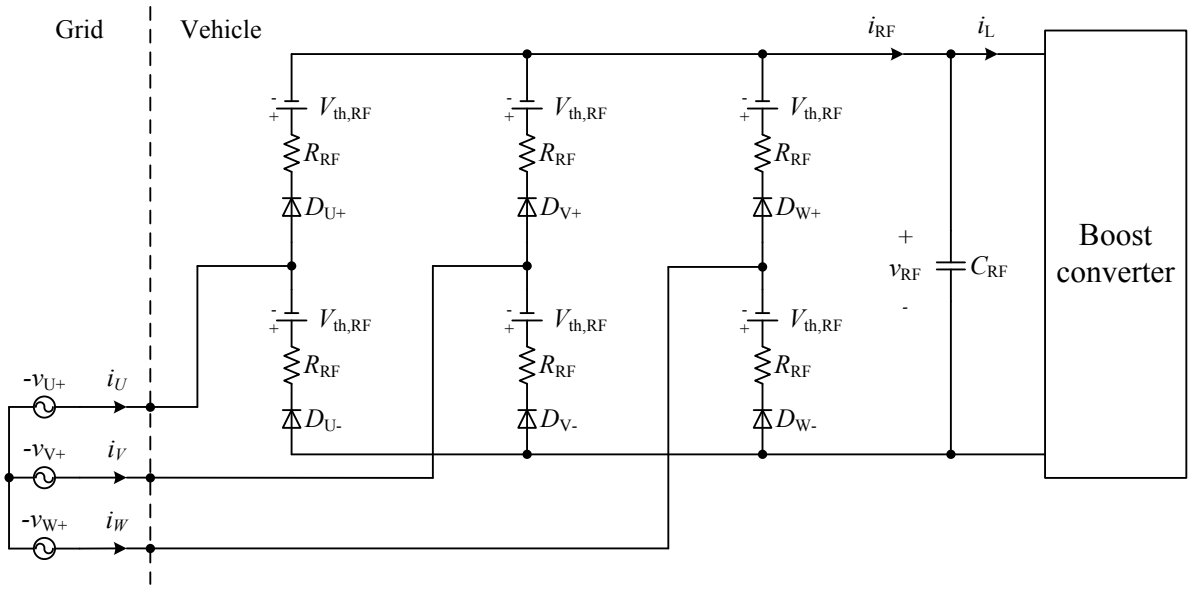

Figure E.1: Circuit diagram of rectifier.

The phase grid voltages are given by

$$v_{\mathrm{U}} = \sqrt{2}V_{\mathrm{p}}\sin(\omega t) \quad [\mathrm{V}] \tag{E.1}$$

$$v_{\mathrm{V}} = \sqrt{2}V_{\mathrm{p}}\sin(\omega t - \frac{2\pi}{3}) \quad [\mathrm{V}] \tag{E.2}$$

$$v_{\mathrm{W}} = \sqrt{2}V_{\mathrm{p}}\sin(\omega t + \frac{2\pi}{3}) \quad [\mathrm{V}] \tag{E.3}$$

where V_{p} [V] RMS phase voltage
ω [rad/s] Electric frequency

If it is assumed that the current to the boost-converter i_{RF} is constant, the phase currents will be constant for $120\,^\circ$ (or $\frac{2\pi}{3}\,\mathrm{rad}$) in each half period as shown in Figure E.2(b).

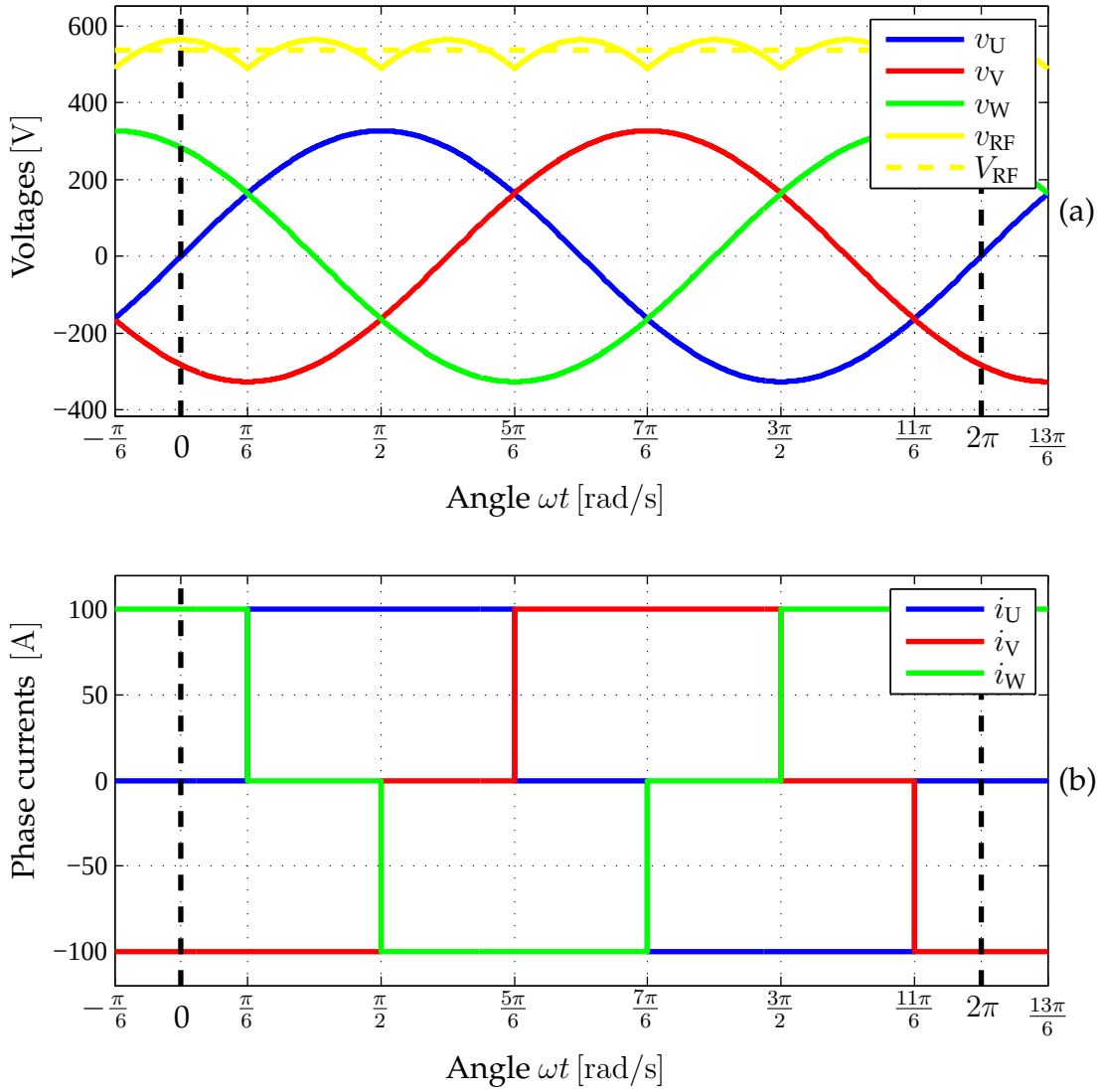

Figure E.2: Voltage and currents of rectifier. (a) Phase voltages and rectified voltage (instantaneous and average). (b) Phase currents

From the figure it can be seen that the current of phase U i_{U} is given by

$$i_{\mathrm{U}} = \begin{cases} 0 & 0 \leq \omega t < \frac{\pi}{6} \\ I_{\mathrm{RF}} & \frac{\pi}{6} \leq \omega t < \frac{5\pi}{6} \\ 0 & \frac{5\pi}{6} \leq \omega t < \frac{7\pi}{6} \\ -I_{\mathrm{RF}} & \frac{7\pi}{6} \leq \omega t < \frac{11\pi}{6} \\ 0 & \frac{11\pi}{6} \leq \omega t < 2\pi \end{cases} \quad [\mathrm{A}] \tag{E.4}$$

The grid RMS-current is therefore

$$I_{\mathrm{Grid}} = \sqrt{\frac{1}{2\pi}\int_0^{2\pi} i_{\mathrm{U}}^2 d\left(\omega t\right)} = I_{\mathrm{RF}}\sqrt{\frac{2}{3}} \quad [\mathrm{A}] \tag{E.5}$$

When the voltage between phase U and V is highest it can be described as

$$\begin{aligned} v_{\mathrm{UV}} &= v_{\mathrm{U}} - v_{\mathrm{V}} = \sqrt{2}V_{\mathrm{p}}\left(\sin(\omega t) - \sin(\omega t - \frac{2\pi}{3})\right) \\ &= \sqrt{2}V_{\mathrm{p}}\left(2\cos(\frac{\omega t + \omega t - \frac{2\pi}{3}}{2})\sin(\frac{\omega t - \omega t + \frac{2\pi}{3}}{2})\right) \\ &= \sqrt{2}\underbrace{\sqrt{3}V_{\mathrm{p}}}_{V_{\mathrm{LL}}}\cos(\omega t - \frac{\pi}{3}) \end{aligned} \quad [\mathrm{V}] \tag{E.6}$$

where V_{LL} [V] Line-line RMS voltage

The rectified voltage is therefore

$$\begin{aligned} v_{\mathrm{RF}} &= v_{\mathrm{UV}} - 2R_{\mathrm{RF}}i_{\mathrm{U}} - 2V_{\mathrm{th,RF}} && \frac{\pi}{6} \leq \omega t < \frac{\pi}{2} \\ &= \sqrt{2}V_{\mathrm{LL}}\cos(\omega t - \frac{\pi}{3}) - 2R_{\mathrm{RF}}I_{\mathrm{RF}} - 2V_{\mathrm{th,RF}} && \frac{\pi}{6} \leq \omega t < \frac{\pi}{2} \end{aligned} \tag{E.7}$$

The rectified voltage v_{RF} repeats itself six times in one phase voltage period. The average rectified voltage is therefore from Equation (E.7) [11]:

$$\begin{aligned} V_{\mathrm{RF}} &= \frac{1}{\frac{\pi}{2} - \frac{\pi}{6}}\int_{\frac{\pi}{6}}^{\frac{\pi}{2}} v_{\mathrm{RF}} d(\omega t) \\ &= \frac{3}{\pi}\int_{\frac{\pi}{6}}^{\frac{\pi}{2}}\left(\sqrt{2}V_{\mathrm{LL}}\cos(\omega t - \frac{\pi}{3}) - 2R_{\mathrm{RF}}I_{RF} - 2V_{\mathrm{th,RF}}\right)d(\omega t) \\ &= \frac{3\sqrt{2}}{\pi}V_{\mathrm{LL}} - 2R_{\mathrm{RF}}I_{\mathrm{RF}} - 2V_{\mathrm{th,RF}} \end{aligned} \quad [\mathrm{V}] \tag{E.8}$$

The average power level P_{RF} of the rectified voltage is therefore

$$P_{\mathrm{RF}} = V_{\mathrm{RF}}I_{\mathrm{RF}} = \underbrace{\frac{3\sqrt{2}}{\pi}V_{\mathrm{LL}}I_{\mathrm{RF}}}_{P_{\mathrm{Grid}}} - \underbrace{\left(2R_{\mathrm{RF}}I_{\mathrm{RF}}^2 + 2V_{\mathrm{th,RF}}I_{\mathrm{RF}}\right)}_{P_{\mathrm{RF,loss}}} \quad [\mathrm{W}] \tag{E.9}$$

where P_{Grid} [W] Power of three phase grid
$P_{\text{loss,RF}}$ [W] Total loss of the rectifier

From Equation (E.5) the grid power can also be written as a function of the grid RMS-current:

$$P_{\text{Grid}} = \frac{3\sqrt{2}}{\pi} V_{\text{LL}} I_{\text{RF}} = \frac{3\sqrt{3}}{\pi} V_{\text{LL}} I_{\text{Grid}} \quad [\text{W}] \tag{E.10}$$

E.1 DESIGN

It is expected that most of the charging of the BEV will take place at the private homes, where the maximum RMS-current is $I_{Grid,max} = 16\,\text{A}$. The maximum grid power and rectifier current are therefore

$$P_{\text{Grid,max}} = \frac{3\sqrt{3}}{\pi} V_{\text{LL}} I_{\text{Grid,max}} = 10.6\,\text{kW} \tag{E.11}$$

$$I_{\text{RF,max}} = \sqrt{\frac{3}{2}} I_{\text{Grid,max}} = 19.6\,\text{A} \tag{E.12}$$

It is assumed that the active rectifier has an efficiency of $\eta_{\text{RF,nom}} = 0.95$ at maximum grid power. The switch-on resistance can therefore be calculated from Equation (E.9):

$$P_{\text{RF,max}} = \eta_{\text{RF,nom}} P_{\text{Grid,max}} = P_{\text{Grid,max}} - \left(2R_{\text{RF}} I_{\text{RF,max}}^2 + 2V_{\text{th,RF}} I_{\text{RF,max}}\right) \quad [\text{W}] \tag{E.13}$$

$$\Updownarrow$$

$$R_{\text{RF}} = \frac{P_{\text{Grid,max}}\left(1 - \eta_{\text{RF,nom}}\right) - 2V_{\text{th,RF}} I_{\text{RF,max}}}{2I_{\text{RF,max}}^2} = 638\,\text{m}\Omega \tag{E.14}$$

F Boost Converter

The line-line RMS-voltage of the grid is $V_{\mathrm{LL}} = 400\,\mathrm{V}$. This is lower than the minimum allowed battery charging voltage of $V_{\mathrm{Bat,max,Base}} N_{\mathrm{Bat,s}} = 525\,\mathrm{V}$. It is therefore necessary to step-up the rectified voltage from the grid. Therefore a boost converter is used as a charger.

The losses of the boost converter are due to the switch resistance $R_{\mathrm{Q,BC}}$ and threshold voltage $V_{\mathrm{Q,th,BC}}$ and the diodes resistance $R_{\mathrm{D,BC}}$ and threshold voltage $V_{\mathrm{D,th,BC}}$. Therefore

$$L\frac{di_{\mathrm{L}}}{dt} = \begin{cases} v_{\mathrm{RF}} - R_{\mathrm{Q,BC}} i_{\mathrm{L}} - V_{\mathrm{Q,th,BC}} & , Q_{\mathrm{BC}} \text{ on} \\ v_{\mathrm{RF}} - R_{\mathrm{D,BC}} i_{\mathrm{L}} - V_{\mathrm{D,th,RF}} - v_{\mathrm{Bat}} & , Q_{\mathrm{BC}} \text{ off} \end{cases} \quad [\mathrm{V}] \quad \text{(F.1)}$$

$$C_{\mathrm{RF}}\frac{v_{\mathrm{RF}}}{dt} = i_{\mathrm{RF}} - i_{\mathrm{L}} \quad [\mathrm{A}] \quad \text{(F.2)}$$

$$C_{\mathrm{Bat}}\frac{dv_{\mathrm{Bat}}}{dt} = \begin{cases} -i_{\mathrm{BC}} & , Q_{\mathrm{BC}} \text{ on} \\ i_{\mathrm{L}} - i_{\mathrm{BC}} & , Q_{\mathrm{BC}} \text{ off} \end{cases} \quad [\mathrm{A}] \quad \text{(F.3)}$$

In steady-state are the derivatives zero. Therefore

$$V_{\mathrm{RF}} = \left(R_{\mathrm{Q,BC}} I_{\mathrm{L}} + V_{\mathrm{Q,th,BC}}\right) D + \left(V_{\mathrm{Bat}} + R_{\mathrm{D,BC}} + V_{\mathrm{D,th,BC}}\right)(1 - D) \quad [\mathrm{V}] \quad \text{(F.4)}$$

$$I_{\mathrm{L}} = I_{\mathrm{RF}} \quad [\mathrm{A}] \quad \text{(F.5)}$$

$$I_{\mathrm{BC}} = I_{\mathrm{L}}\,(1 - D) \quad [\mathrm{A}] \quad \text{(F.6)}$$

In order to simplify it is assumed that the resistances and threshold voltages of the switch Q_{BC} and diode D_{BC} are equal, i.e. $R_{\mathrm{BC}} = R_{\mathrm{Q,BC}} = R_{\mathrm{D,RF}}$ and $V_{\mathrm{th,BC}} = V_{\mathrm{Q,th,BC}} = V_{\mathrm{D,th,BC}}$. Equation (F.4) is therefore reduced to

$$V_{\mathrm{RF}} = R_{\mathrm{BC}} I_{\mathrm{L}} + V_{\mathrm{th,BC}} + V_{\mathrm{Bat}}\,(1 - D) \quad [\mathrm{V}] \quad \text{(F.7)}$$

The power equation of the boost converter is therefore given by

$$\underbrace{V_{\mathrm{RF}} I_{\mathrm{RF}}}_{P_{\mathrm{RF}}} = \underbrace{V_{\mathrm{Bat}} I_{\mathrm{BC}}}_{P_{\mathrm{BC}}} + \underbrace{R_{\mathrm{BC}} I_{\mathrm{RF}}^2 + V_{\mathrm{th,BC}} I_{\mathrm{RF}}}_{P_{\mathrm{Loss,BC}}} \quad [\mathrm{W}] \quad \text{(F.8)}$$

F.1 Design

It is also assumed that the boost converter has efficiency $\eta_{\mathrm{BC,nom}} = 0.95$ at the maximum power. The maximum power of the boost converter is therefore

$$P_{\mathrm{BC,max}} = P_{\mathrm{RF,max}} \eta_{\mathrm{BC,nom}} \quad [\mathrm{W}] \quad \text{(F.9)}$$

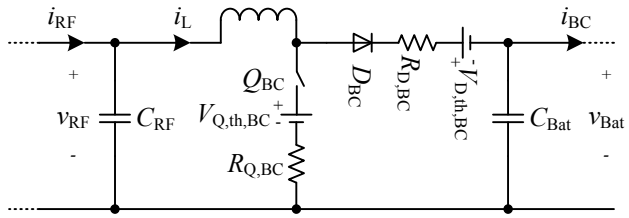

Figure F.1: Circuit diagram of boost converter.

The threshold voltage is $V_{\text{th,BC}} = 1\,\text{V}$. From Equation (F.8) the resistance of the boost converter is therefore

$$P_{\text{RF,max}} = \eta_{\text{BC,nom}} P_{\text{RF,max}} + R_{\text{BC}} I_{RF,max}^2 + V_{\text{th,BC}} I_{\text{RF,max}} \quad [\text{W}] \tag{F.10}$$

$$\Updownarrow$$

$$R_{\text{BC}} = \frac{P_{\text{RF,max}} \left(1 - \eta_{\text{BC,rat}}\right) - V_{\text{th,BC}} I_{\text{RF,max}}}{I_{\text{RF,max}}^2} = 1.33\,\Omega \tag{F.11}$$

G Braking Resistor

During the regenerative braking is the maximum allowed charging current of the battery $i_{\text{Bat,max,cha}}$ given by

$$i_{\text{Bat,max,cha}} = N_{\text{Bat,p}} \frac{V_{\text{Bat,max,Base}} - v_{\text{Bat,int,Base}}}{R_{\text{Bat,Base,cha}}} \quad [\text{A}] \tag{G.1}$$

where

$N_{\text{Bat,p}}$	$[-]$	Number of parallel strings
$V_{\text{Bat,max,Base}}$	$[\text{V}]$	Maximum cell charging voltage
$v_{\text{Bat,int,Base}}$	$[\text{V}]$	Internal cell voltage
$R_{\text{Bat,Base,cha}}$	$[\Omega]$	Cell charging resistance

Ideally should the battery handle all the current from the different devices. The reference battery current is therefore

$$i^*_{\text{Bat}} = i_{\text{Aux}} + i_{\text{Inv}} - i_{\text{BC}} \quad [\text{A}] \tag{G.2}$$

In order to make sure that the critical cell voltage $V_{\text{Bat,max,Base}}$ not is exceeded are the battery and braking resistor currents therefore given by

$$i_{\text{Bat}} = \begin{cases} i^*_{\text{Bat}} & , \quad -i^*_{\text{Bat}} < i_{\text{Bat,max,cha}} \\ -i_{\text{Bat,max,cha}} & , \quad -i^*_{\text{Bat}} \geq i_{\text{Bat,max,cha}} \end{cases} \quad [\text{A}] \tag{G.3}$$

$$i_{\text{BR}} = i_{\text{Bat}} - i^*_{\text{Bat}} \quad [\text{A}] \tag{G.4}$$

The negative sign in front of i^*_{Bat} in Equation (G.3) is due to the sign convention of the battery. A discharging current is defined as a positive battery current. The power of the braking resistor is given by

$$p_{\text{BR}} = v_{\text{Bat}} i_{BR} \tag{G.5}$$

The rated power of the braking resistor is the maximum power through it, i.e.

$$P_{\text{BR,rat}} = \max\left(p_{\text{BR}}\right) \quad [\text{W}] \tag{G.6}$$

H Fuel Cell Modeling

In this appendix a Low Temperature Proton Exchange Membrane Fuel Cell (LT-PEMFC) will be modeled. The parameters will be extracted from data sheet specifications.

H.1 Specifications and Characteristics

The modeling is based on a Ballard fuel cell stack (FCgen-1020ACS) which consist of 56 series connected cells. The specifications can be seen in Table H.1.

Manufacture	Ballard
Type	FCgen-1020ACS
Temperature range	$-20\,^{\circ}\mathrm{C}$ to $52\,^{\circ}\mathrm{C}$
Cells $N_{\mathrm{FC,cell}}$	56
Nominal voltage $V_{\mathrm{FC,nom,cell}}$	$0.642\,\mathrm{V}$
Open circuit voltage $V_{\mathrm{FC,max,cell}}$	$1.0\,\mathrm{V}$
Nominal current $I_{\mathrm{FC,cell}}$	$65\,\mathrm{A}$
Stack mass $\mathrm{Mass}_{\mathrm{FC,stack,Base}}$	$11\,\mathrm{kg}$
Mass $M_{\mathrm{FC,cell}}$	$0.196\,\mathrm{kg}$
Stack volume $\mathrm{Vol}_{\mathrm{FC,stack}}$	$13.1\,\mathrm{L}$
Volume $\mathrm{Vol}_{\mathrm{FC,cell}}$	$0.234\,\mathrm{L}$
Cost $\mathrm{CE}_{\mathrm{FC}}$ (2010 prediction [7])	$500\,\$/\mathrm{kW}$
Storage cost $\mathrm{CM}_{\mathrm{sto}}$ (estimated from [7])	$700\,\$/(\mathrm{kgH2})$
Storage energy density $\mathrm{ED}_{\mathrm{sto}}$ [10]	$1.5\,\mathrm{kWh/L}$
Storage specific energy $\mathrm{SE}_{\mathrm{sto}}$ [10]	$2\,\mathrm{kWh/kg}$

Table H.1: Data sheet specifications of Ballard FCgen-1020ACS fuel cell stack [1].

H.2 Polarization Curve Modeling

In Figure H.1 the polarization curve of a single fuel cell can be seen.

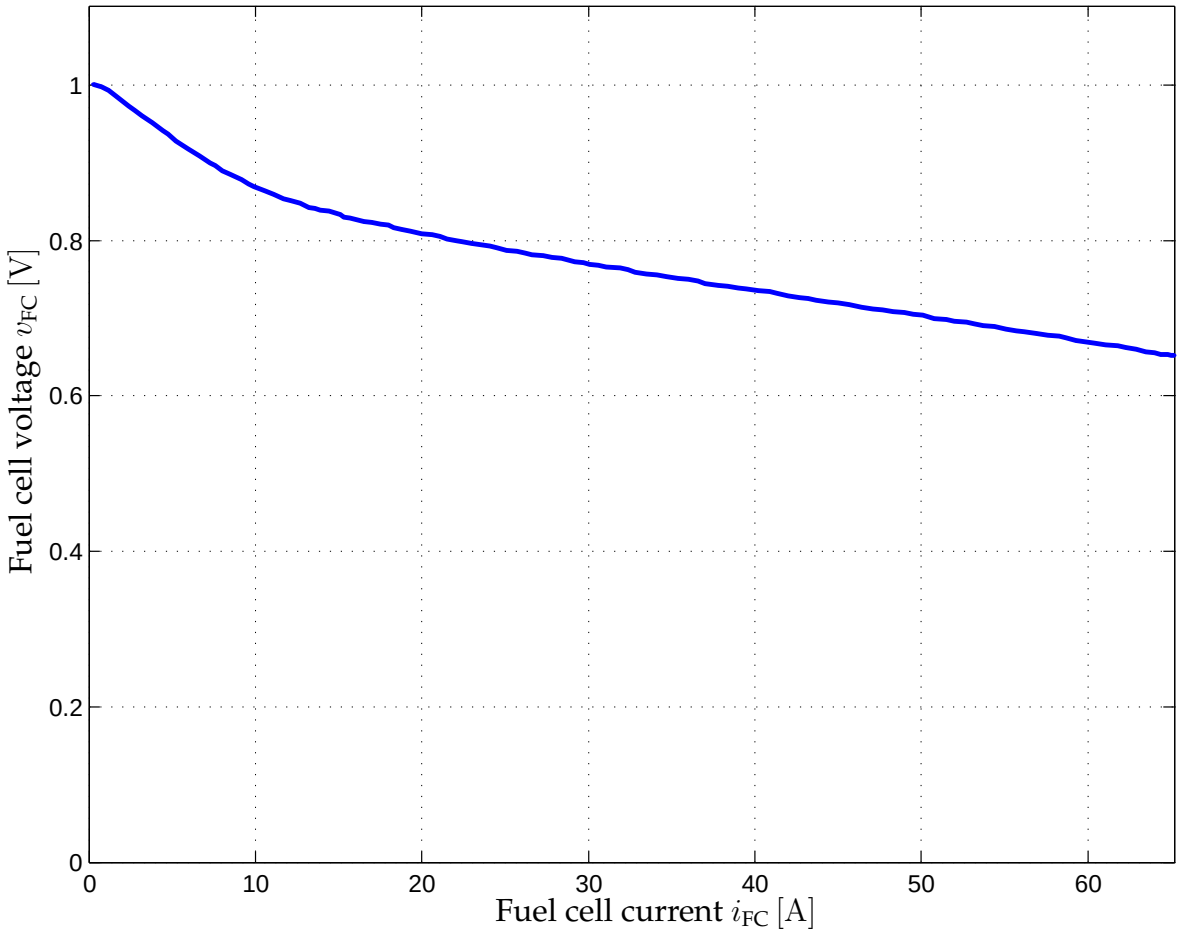

Figure H.1: Per cell polarization curve of Ballard FCgen-1020ACS fuel cell stack.

H.3 EFFICIENCY MODELING

The fuel cell efficiency is calculated by the current in per unit, i.e.

$$i_{\text{FC,pu}} = \frac{i_{\text{FC}}}{i_{\text{FC,max}}} \qquad [-] \qquad \text{(H.1)}$$

$$\begin{aligned} \eta_{\text{FC}} = & -2.86921829 \cdot i_{\text{FC,pu}}^4 + 8.74517883 \cdot i_{\text{FC,pu}}^3 \\ & - 9.55224805 \cdot i_{\text{FC,pu}}^2 + 4.08022346 \cdot i_{\text{FC,pu}} \end{aligned} \qquad [-] \qquad \text{(H.2)}$$

In Figure H.2 the efficiency curve of the fuel cell can be seen.

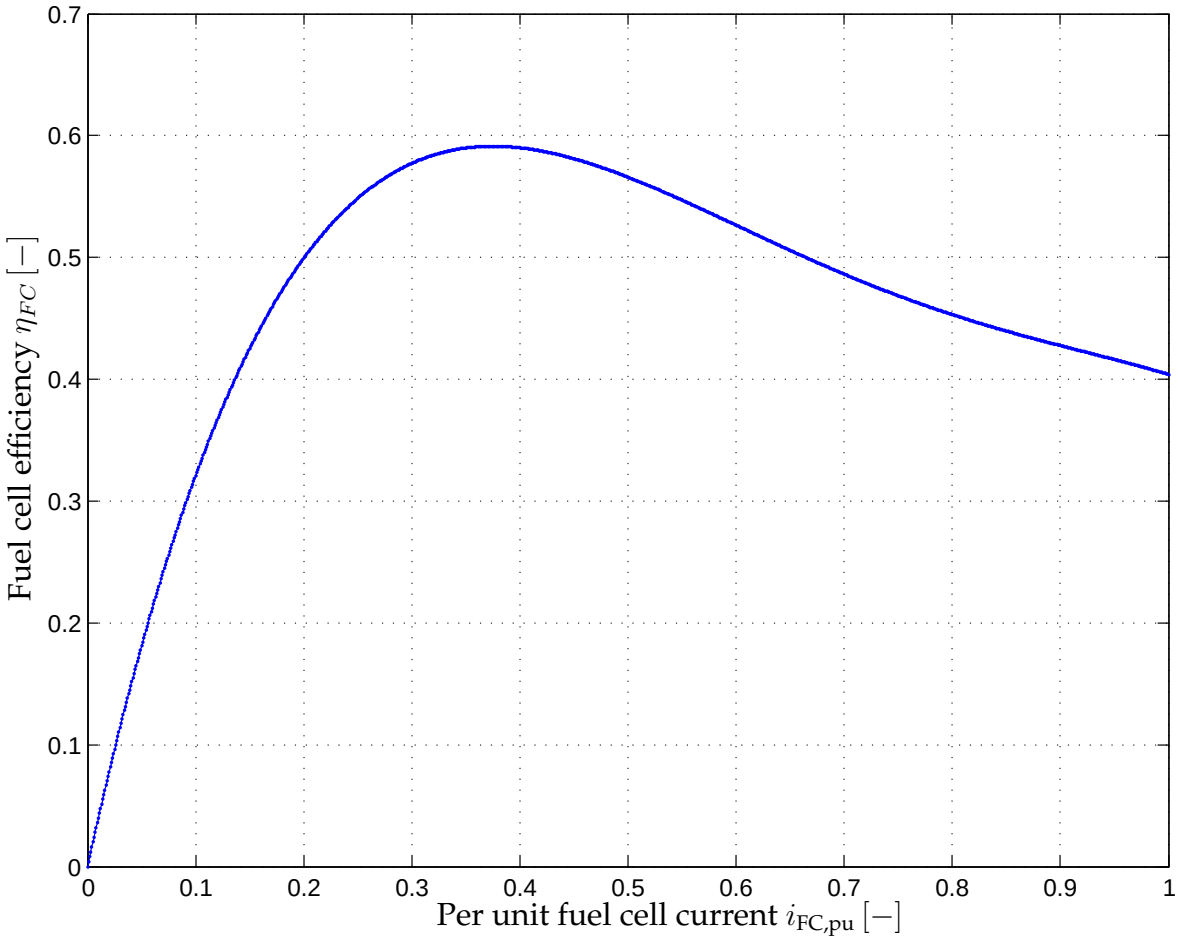

Figure H.2: Fuel cell efficiency as a function of the per unit fuel cell current.